Plant mRNAs move into a fungal pathogen via extracellular vesicles to reduce infection

Wang, Shumei; He, Baoye; Wu, Huaitong; Cai, Qiang; Ramírez-Sánchez, Obed; Abreu-Goodger, Cei

Published in:
Cell Host & Microbe

DOI:
10.1016/j.chom.2023.11.020

Publication date:
2023

Article

Cell Host & Microbe

Plant mRNAs move into a fungal pathogen via extracellular vesicles to reduce infection

Graphical abstract

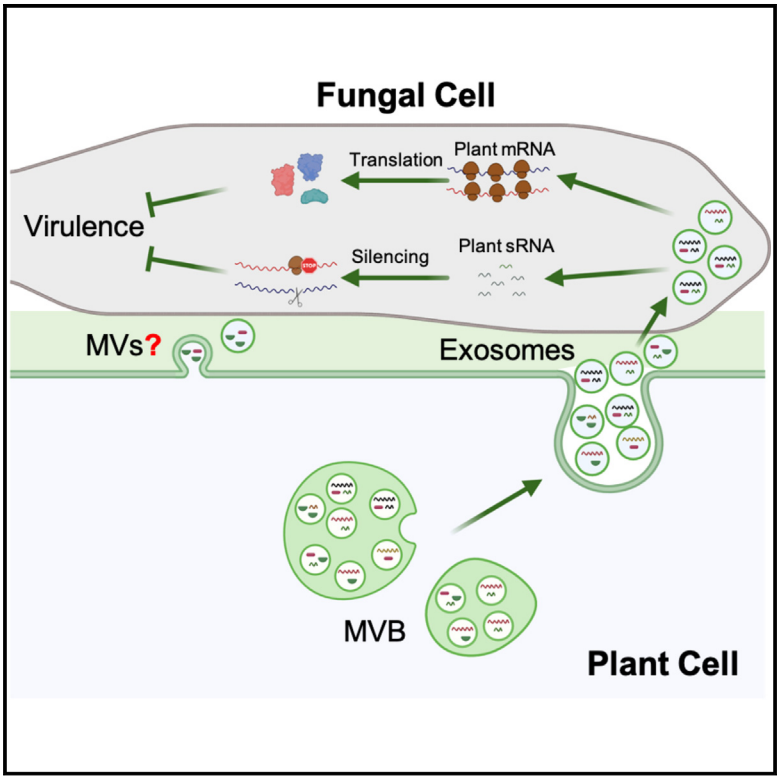

Authors

Shumei Wang, Baoye He, Huaitong Wu, ..., Cei Abreu-Goodger, Paul R.J. Birch, Hailing Jin

Correspondence

hailingj@ucr.edu

In brief

Exchange of small RNAs between host plants and their pathogens modulates gene expression in the interacting partners during host-pathogen interactions. Wang et al. show that the model plant *Arabidopsis* also delivers mRNAs within extracellular vesicles into fungal pathogen cells where they are translated and function to reduce infection.

Highlights

- *Arabidopsis* delivers mRNAs via extracellular vesicles into fungal pathogen cells
- Delivered host mRNAs are translated within fungal cells
- Proteins translated from delivered host mRNAs reduce fungal infection
- Knockouts in host genes corresponding to delivered mRNAs are more susceptible

Wang et al., 2024, Cell Host & Microbe *32*, 1–13
January 10, 2024
https://doi.org/10.1016/j.chom.2023.11.020

CellPress

Cell Host & Microbe

CellPress
OPEN ACCESS

Article

Plant mRNAs move into a fungal pathogen via extracellular vesicles to reduce infection

Shumei Wang,[1] Baoye He,[1] Huaitong Wu,[1] Qiang Cai,[2] Obed Ramírez-Sánchez,[3] Cei Abreu-Goodger,[4] Paul R.J. Birch,[5,6] and Hailing Jin[1,7,*]

[1]Department of Microbiology and Plant Pathology, Center for Plant Cell Biology, Institute for Integrative Genome Biology, University of California, Riverside, Riverside, CA, USA
[2]State Key Laboratory of Hybrid Rice, College of Life Science, Wuhan University, Wuhan, China
[3]National Laboratory of Genomics for Biodiversity (Langebio), Cinvestav, Irapuato 36821 Guanajuato, Mexico
[4]Institute of Ecology and Evolution, School of Biological Sciences, the University of Edinburgh, Edinburgh EH9 3FL, UK
[5]Division of Plant Sciences, School of Life Science, University of Dundee at James Hutton Institute, Invergowrie, Dundee DD2 5DA, UK
[6]Cell and Molecular Sciences, James Hutton Institute, Invergowrie, Dundee DD2 5DA, UK
[7]Lead contact
*Correspondence: hailingj@ucr.edu
https://doi.org/10.1016/j.chom.2023.11.020

SUMMARY

Cross-kingdom small RNA trafficking between hosts and microbes modulates gene expression in the interacting partners during infection. However, whether other RNAs are also transferred is unclear. Here, we discover that host plant *Arabidopsis thaliana* delivers mRNAs via extracellular vesicles (EVs) into the fungal pathogen *Botrytis cinerea*. A fluorescent RNA aptamer reporter Broccoli system reveals host mRNAs in EVs and recipient fungal cells. Using translating ribosome affinity purification profiling and polysome analysis, we observe that delivered host mRNAs are translated in fungal cells. Ectopic expression of two transferred host mRNAs in *B. cinerea* shows that their proteins are detrimental to infection. *Arabidopsis* knockout mutants of the genes corresponding to these transferred mRNAs are more susceptible. Thus, plants have a strategy to reduce infection by transporting mRNAs into fungal cells. mRNAs transferred from plants to pathogenic fungi are translated to compromise infection, providing knowledge that helps combat crop diseases.

INTRODUCTION

Host-microbe interactions represent a molecular battleground involving exchanges of diverse classes of biomolecules.[1–3] Although toxins, metabolites, and proteins are transferred between hosts and microbes during infection,[2,3] transfer of RNAs is less well understood. Small RNAs (sRNAs) are a class of short non-coding RNAs that can induce silencing of target genes with sequence complementarity.[4] Recent discoveries show that some microbes deliver sRNAs into host cells and hijack host Argonaute (AGO) proteins to silence host genes for successful infection, a process named "cross-kingdom RNAi."[5–9] During the co-evolutionary arms race between hosts and microbes, hosts also transfer sRNAs into interacting microbes to silence virulence-related genes in pathogens.[1,10–12] However, it is unknown whether other classes of RNA molecules, such as messenger RNAs (mRNAs), can also move from hosts to interacting microbes.

Extracellular vesicles (EVs) are a diverse group of cell-derived membranous structures that are released into the extracellular environment. EVs contain a cargo of various biomolecules, including proteins, lipids, nucleic acids (such as RNA and DNA), and metabolites.[13] They serve as important mediators of intercellular communication by transferring biological molecules, thereby influencing various physiological and pathological processes in diverse organisms.[14] In animals, EVs have gained significant attention in the scientific and medical communities due to their potential as diagnostic and therapeutic tools.[14] In plants, EVs play an important role in protecting sRNA during trafficking from hosts to interacting microbes to the detriment of pathogen infection.[10,15] Strikingly, fungal pathogen *Botrytis cinerea*, which causes gray mold disease on more than 1,400 plant species,[16] uses a similar strategy as its plant host to also deploy EVs to protect and transport sRNA effectors into host cells for cross-kingdom RNAi.[17]

mRNA conveys genetic information within cells that are usually translated into proteins to fulfill its biological function. Intercellular and systemic mRNA trafficking within an organism has been reported in animals and plants.[18–21] In animals, EVs are important for intercellular and systemic sRNA and mRNA trafficking within an organism.[18,22–24] Recently, the fungal pathogen of maize, *Ustilago maydis*, was shown to secrete EVs containing mRNAs, which may participate in regulating plant-pathogen interactions.[25] However, it is currently unclear whether plant EVs can transport mRNAs and other classes of RNA molecules aside from sRNAs. Critically, if mRNAs can move from plants to

interacting microbes, are they translated in the microbes and what is the potential consequence to pathogen fitness and infectivity?

Here, our findings demonstrate that EVs transport plant mRNAs to interacting pathogenic fungal cells. Importantly, we observed that these transferred host mRNAs are associated with fungal polysomes for translation, with the potential to compromise infection. These discoveries inform potential future strategies for effectively controlling plant diseases.

RESULTS

Plant EVs carry mRNAs

To investigate whether plant mRNAs are associated with EVs during infection, we conducted an mRNA profiling analysis on purified EVs (P100 fraction: ultracentrifugation at 100,000 × g) from leaf apoplastic wash fluids (AWFs) collected early (16 h) in the interaction between *Botrytis cinerea* and *Arabidopsis* leaves and uninfected leaves (mock) as described in Huang et al.[26] The time point of 16 h post-*B. cinerea* infection (hpi) is recognized to be during the early biotrophic phase of infection before any host cell death occurs,[27] and no dead host cells were observed after the trypan blue staining (Figure S1A). The quality of the AWFs from infected plant leaves was evaluated before 100,000 × g ultracentrifugation by western blot analysis to measure the potential contamination of chloroplasts, mitochondria, and their fragments from cell leakage and death. The chloroplast membrane protein Tic40 and mitochondrial inner membrane protein Tim17 were not detected in the AWF fraction (Figure S1B).[28,29] The quality of EVs was further monitored by transmission electron microscopy (TEM) and nanoparticle-tracking analysis (Figures S1C and S1D). Using 100 normalized reads per kilobase of transcript per million mapped reads (RPKM) in each biological repeat as a cutoff, a total of 567 *Arabidopsis* transcripts were identified in the EV samples from 16 hpi samples (EV_infected) and nearly 30% of them were induced after infection compared with the EVs isolated from uninfected leaves (Tables S1 and S2). Gene ontology (GO) analysis revealed that 228 of the 567 (40.2%) EV-associated *Arabidopsis* mRNAs encode genes associated with biotic stress or defense responses with a clear enrichment of genes involved in detoxification, response to reactive oxygen species, defense response to fungus, hormone metabolic process, secondary metabolic process, and immune response, etc. (Figure S1E; Table S1), whereas biotic stress or defense responses associated genes only represent 11% of the total genes in the *Arabidopsis* genome.[30] Notably, the protein products of 167 EV-associated mRNAs (29% of 567 genes) could be found in mitochondrial proteomes (Table S1) according to the subcellular location database for *Arabidopsis* proteins (SUBA4, http://suba.live). This represents an almost 4-fold enrichment compared with the percent of mitochondria-localized protein genes in the entire *Arabidopsis* genome (7.4%).[31] RNA-seq analysis on total mRNAs from *Botrytis*-infected *Arabidopsis* leaves was performed for comparative analysis (Table S3). The profiles of EV-associated mRNAs were distinct from the total mRNA profiles; for example, considering the 100 most abundant *Arabidopsis* mRNAs in each dataset in the libraries generated from infected plants, only 33 were shared (Table S3). This suggests that transcript abundance in leaf cells does not directly explain transcript abundance in EVs.

We experimentally validated a selection of EV-mRNA candidates of various lengths that have potential roles in plant defense or stress responses, in addition to their developmental roles of some genes. The full-length mRNA transcripts (open reading frame) of 15 candidates were detected in the purified EV P100 fraction (Figure 1A). Transcripts abundant in total mRNA and absent in the EV dataset (Table S3), *Outer Envelope Protein 6* (*OEP6*), *General Regulatory Factor 10* (*GRF10*), and *Profilin* 5 (*PRO5*), were used as negative controls (Figure 1A). We chose four *Arabidopsis* transcripts for further characterization from the EV dataset that are induced during infection and, in addition to their known functions in uninfected plants, could thus play a role in plant immunity: *Senescence-associated gene 21* (*SAG21*),[32] *ATP sulfurylase 1* (*APS1*),[33,34] *Peroxiredoxin IIC* (*PRXIIC*),[35] and *Hevein-like* (*HEL*).[36] The full-length transcripts of these genes were still detected in purified EVs after micrococcal nuclease and proteinase K digestion unless the vesicles were first ruptured with Triton X-100 (Figure 1B), demonstrating that these mRNAs are indeed contained within the vesicles rather than bound to the outer surface or associated with independent protein aggregates.

Plants produce different classes of EVs based on their biogenesis pathways and specific protein markers.[37,38] We previously showed that Tetraspanin (TET)-positive EVs (considered plant exosomes), especially TET8- and TET9-positive EVs, are mainly responsible for sRNA transport from plants to fungal pathogens.[10] The *tet8* mutant shows fewer EVs under TEM[10,39] and has impaired immune responses against fungal infection.[10] To determine whether plant mRNAs are transported by TET8-positive EVs, we examined the levels of selected EV-mRNAs in immuno-captured TET8-positive exosome fractions purified using a TET8-specific antibody.[15,26] Specificity of the immuno-isolation was verified using an independent control antibody (IgG). Full-length transcripts of *SAG21*, *APS1*, *PRXIIC*, and *HEL* were detected in the immuno-captured TET8-exosome fractions, but not in the IgG control (Figure 1C). Moreover, the transcripts of these genes were barely detectable in EVs from the *tet8/tet9* double (*tet8* knockout and *tet9* knockdown) mutant[10] compared with EVs prepared from wild-type *Arabidopsis* (Figure 1C). Together, these results confirm that plant exosomes also carry mRNAs in addition to sRNAs.

Plant mRNAs are observed in EVs

To visualize the mRNAs in host EVs, we applied an improved RNA reporter system using a fluorescent RNA aptamer, Three-Way Junction-4 x Broccoli (3WJ-4xBro), which was optimized for RNA imaging in plant cells.[40,41] Here, we tagged full-length *SAG21*, *APS1*, *PRXIIC*, and *HEL* transcripts with *3WJ-4xBro* aptamer, which allowed the tagged mRNA transcripts to be directly observed in TET8-positive EVs when co-expressed with TET8-mCherry in *Nicotiana benthamiana* cells (Figures 2A–2C and S2A), whereas the negative control, *OEP6-3WJ-4xBro*, was not detectable in EVs (Figures 2A–2C). The full-length *SAG21*-, *APS1*-, *PRXIIC*-, and *HEL-3WJ-4xBro* fusion transcripts were also detected in purified EVs from *N. benthamiana* (Figure S2B).

For further in-depth functional analysis, we selected two genes, *SAG21* and *APS1*. Both SAG21 and APS1 can be

Please cite this article in press as: Wang et al., Plant mRNAs move into a fungal pathogen via extracellular vesicles to reduce infection, Cell Host & Microbe (2023), https://doi.org/10.1016/j.chom.2023.11.020

CellPress
OPEN ACCESS

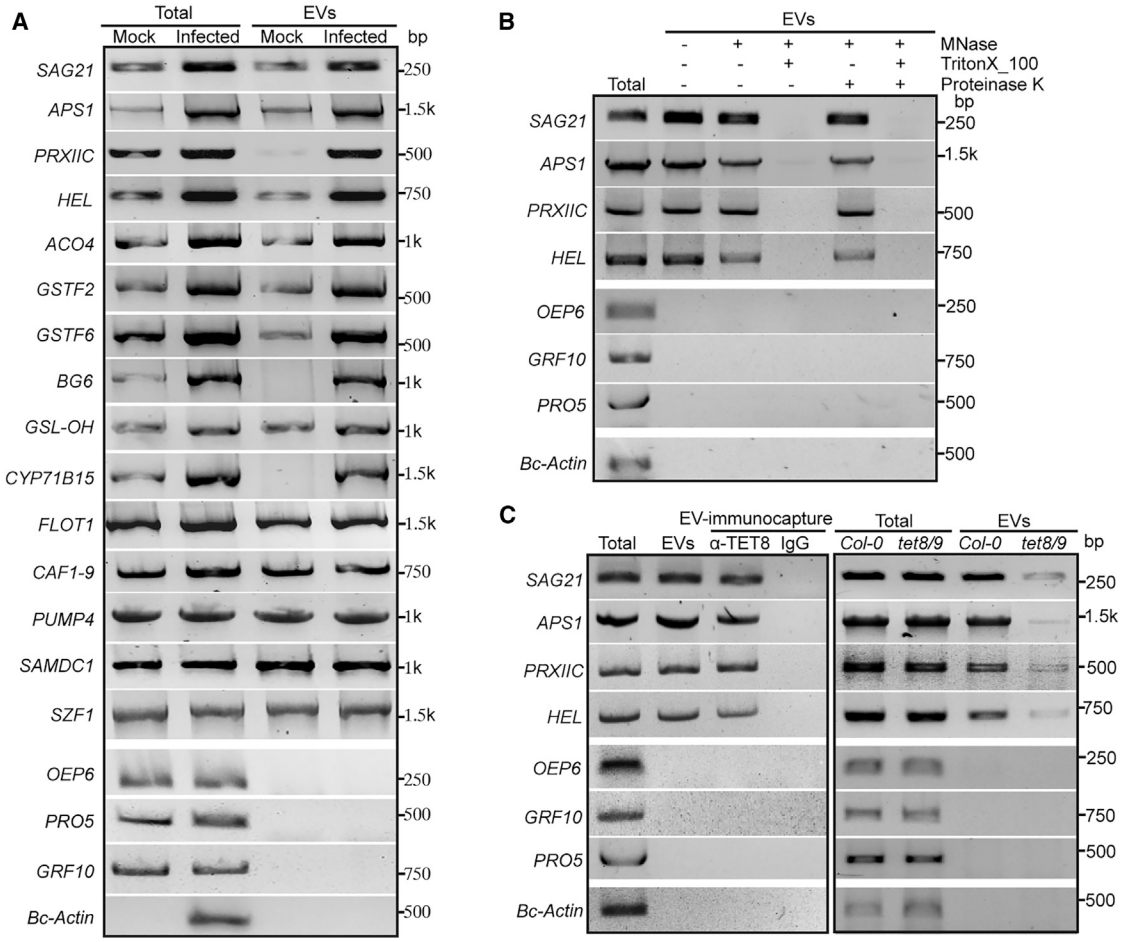

Figure 1. Plant EVs carry mRNAs

(A) Full-length plant transcripts were detected by RT-PCR in EVs isolated from mock-treated and *B. cinerea*-infected *Col-0* leaves. Total RNAs from mock and infected leaves were used as controls.

(B) Full-length host transcripts were detected by RT-PCR after micrococcal nuclease and proteinase K digestion, indicating that they are inside the EVs. Treatments are as indicated (+).

(C) Full-length plant transcripts were detected in TET8-positive exosomes by RT-PCR. EVs were isolated from *Arabidopsis* leaves infected by *B. cinerea*. TET8-positive exosomes were obtained by immunocapture with a TET8-specific antibody from isolated EVs of the P100 fraction. IgG non-specific antibody was used as a control. The same transcripts were only weakly detected in a *tet8/tet9* double mutant line. *OEP6*, *PRO5*, and *GRF10* were used as negative controls. *Bc-actin* was used as a pathogen control gene, which was only detected in infected *Col-0* leaves (Total) (A–C). DNA size markers are in base pairs (bp) (A–C). See also Figure S1 and Tables S1–S3.

targeted to plant mitochondria,[31] and APS1 possesses a dual-targeting signal directing it to both mitochondria and chloroplasts.[42] *SAG21* is induced by the infection of *B. cinerea*, numerous bacterial, fungal, and oomycete pathogens, pathogen elicitors, oxidative stress, and plant defense hormones such as salicylic acid, methyl jasmonate, and ethylene.[32,43] Transgenic plants overexpressing *SAG21* exhibit less susceptibility to the infection of *B. cinerea* and bacterial pathogen *Pseudomonas syringae pv. tomato DC3000*.[32] *APS1* is also induced by *B. cinerea*, oomycete pathogen *Phytophthora infestans*, and oxidative stress.[43] APS1 participates in the biosynthesis of essential metabolites, including glucosinolates, which are toxic to fungal cells.[33,34,44] However, there is no direct evidence that APS1 participates in the defense response to *B. cinerea* infection. We generated stable transgenic *Arabidopsis* plants expressing full-length *SAG21-3WJ-4xBro*, *APS1-3WJ-4xBro*, or control *OEP6-3WJ-4xBro*, and these transgenic lines did not show any obvious developmental difference from the wild type. Quantitative RT-PCR and confocal microscopy revealed that all fusion transcripts were expressed and detected in plant cells (Figures S2C and S2D). As expected, only *SAG21-3WJ-4xBro* and *APS1-3WJ-4xBro* transcripts, but not *OEP6-3WJ-4xBro*, were observed in the purified EV P100 fraction from uninfected plants (Figures 2D–2F). The full-length transcripts of tagged *SAG21* and *APS1* were also detected (Figure S2E). These findings provide direct evidence that plant EVs carry specific mRNAs.

Plant mRNAs are transported into fungal cells

To determine whether these EV-associated plant mRNAs can be delivered into interacting fungal cells during infection, we

Please cite this article in press as: Wang et al., Plant mRNAs move into a fungal pathogen via extracellular vesicles to reduce infection, Cell Host & Microbe (2023), https://doi.org/10.1016/j.chom.2023.11.020

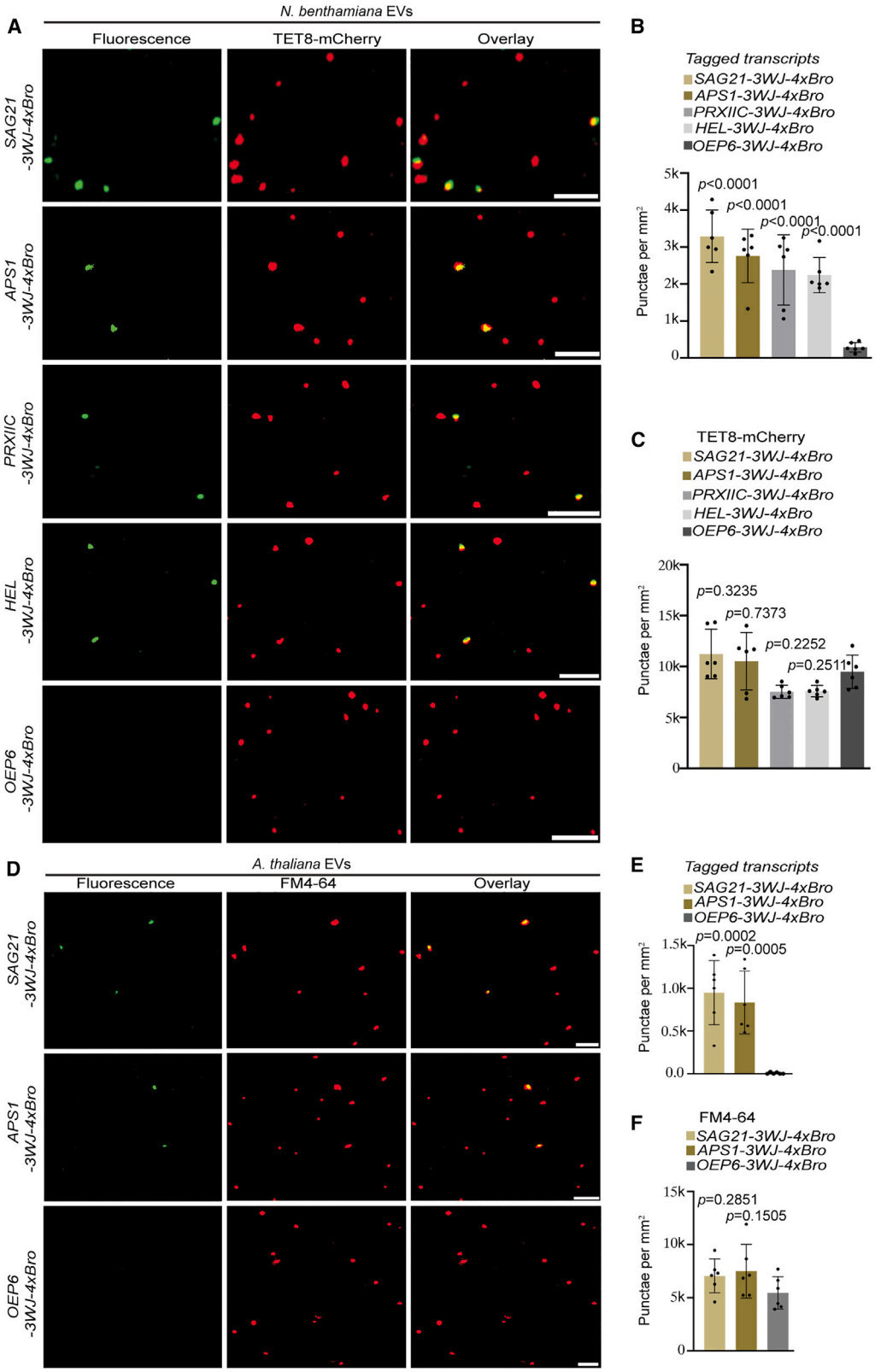

(legend on next page)

Please cite this article in press as: Wang et al., Plant mRNAs move into a fungal pathogen via extracellular vesicles to reduce infection, Cell Host & Microbe (2023), https://doi.org/10.1016/j.chom.2023.11.020

isolated pure *B. cinerea* cells from infected *Arabidopsis* leaves using a sequential protoplasting strategy as reported in Cai et al.[10,45] Cultured *B. cinerea* mixed with uninfected leaves was subjected to the same procedure as a negative control to exclude potential contamination during the experimental procedure. The full-length EV-associated plant mRNAs (*SAG21*, *APS1*, *PRXIIC*, and *HEL*) were detected in *B. cinerea* cells isolated from infected leaves (Figure 3A), indicating that these mRNAs are taken up by fungal cells. In contrast, transcripts not associated with EVs (*OEP6*, *PRO5*, and *GRF10*) were not detected in fungal cells, as anticipated (Figure 3A). None of the plant transcripts that were detected in fungal cells after infection were detected in the negative control of cultured *B. cinerea* cells mixed with uninfected *Arabidopsis* leaves right before the fungal cell isolation (Figure 3A). This result shows that full-length EV-associated plant mRNAs are indeed transferred into fungal cells during infection. We also examined the levels of *SAG21*, *APS1*, *PRXIIC*, and *HEL* in *B. cinerea* cells isolated from infected *tet8/tet9* leaves. Fewer EV-associated transcripts were detected in *B. cinerea* cells isolated from *tet8/tet9* than *Col-0* (Figure 3A), indicating that plant exosomes play an important role in the transport of plant mRNAs into fungal cells.

To further test the involvement of plant EVs in cross-kingdom mRNA trafficking into fungal cells, *Arabidopsis* EVs were isolated from the transgenic lines expressing *3WJ-4xBro*-tagged *SAG21*, *APS1*, or *OEP6* and incubated with *in vitro* cultured *B. cinerea* conidia for 4 h. After incubation, the full-length transcripts of *SAG21-3WJ-4xBro* and *APS1-3WJ-4xBro*, but not *OEP6-3WJ-4xBro*, were detected in purified *B. cinerea* cells (Figure 3B). The fluorescence of *SAG21-3WJ-4xBro* and *APS1-3WJ-4xBro* transcripts, but not *OEP6-3WJ-4xBro*, was observed in fungal hyphae after incubation with EVs prepared from uninfected transgenic plants expressing corresponding *3WJ-4xBro*-tagged transcripts (Figures 3C and 3D). These results support the hypothesis that plant mRNAs are transported by EVs into fungal cells.

To test whether we can also observe plant mRNA transcripts inside fungal cells during natural infection, *B. cinerea* cells were isolated from infected *3WJ-4xBro*-tagged transgenic *Arabidopsis*. As expected, we found fungal cells showing fluorescence of *SAG21-3WJ-4xBro* or *APS1-3WJ-4xBro* and detected the full-length tagged transcripts of *SAG21* and *APS1* in fungal cells (Figures 3E–3G). The tagged *OEP6* transcript from the negative control *OEP6-3WJ-4xBro* was not detected. These results confirmed that plant mRNAs are indeed entering fungal cells during natural infection.

Plant mRNAs are translated in fungal cells

As most mRNAs are translated into proteins to perform biological functions, we asked whether these transferred plant mRNAs can be translated into proteins after entering fungal cells. We adopted the translating ribosome affinity purification followed by RNA-seq (translating ribosome affinity purification [TRAP]-seq) method, which is an effective way to identify actively translated mRNAs.[46,47] We generated a *B. cinerea* transformant strain expressing yellow fluorescent protein (YFP)-tagged *B. cinerea* Ribosome Protein Large subunit 23 (BcRPL23-YFP), a subunit presents at the surface of the Ribosome complex.[48] This strain exhibits similar growth and infection phenotype as the wild-type strain and allows pulling down all the mRNAs associated with fungal ribosomes. TRAP-seq analysis was performed to isolate and sequence *B. cinerea* ribosome-associated mRNAs from BcRPL23-YFP cells during *Arabidopsis* infection (TRAP_infected). Cultured hyphae of the *B. cinerea* transformant mixed with uninfected *Arabidopsis Col-0* leaves were used as a control (TRAP_mix) to exclude potential contamination during the experimental procedure. A total of 320 plant protein-coding mRNAs were associated with fungal ribosomes in all three biological replicates with at least 50 RPKM (considering only reads mapping to *Arabidopsis*) and >3-fold change (TRAP_infected/mix) as a cutoff (Table S4A). Consistent with the proposed mechanism of EV-mediated transfer, 63% (201) of 320 TRAP-associated genes overlapped with the mRNAs identified in EVs (Table S4B). GO analysis revealed that defense response-related genes were highly enriched in the *Botrytis* BcRPL23 TRAP gene list (Figure S3A). Strikingly, 128 of the 201 genes (64%) present in both TRAP- and EV-associated gene lists are biotic stress- or defense response-related. Again, 72 of the TRAP-associated genes (23%) encode proteins that are present in mitochondrial proteomes,[31] 48 of them (67%) overlap with transcripts encoding mitochondria-targeted proteins in EVs (Figure S3B). It is worth noting that abundant chloroplast-genome-derived mRNAs and nuclear-photosynthesis-associated mRNAs are not enriched in the TRAP dataset, indicating that there is no significant contamination with abundant host cellular transcripts. The full-length transcripts of plant EV-associated mRNAs *SAG21*, *APS1*, *PRXIIC*, and *HEL* were detected by RT-PCR after BcRPL23-YFP pull-down from infected samples but not from the control samples in which *in vitro* cultured *B. cinerea* hyphae were mixed with uninfected *Arabidopsis* (Figure 4A). This is consistent with the hypothesis that these plant mRNAs can be transferred to *Botrytis* and become associated with fungal ribosomes.

Figure 2. Plant mRNAs are observed in EVs

(A) Confocal images of EVs isolated from *N. benthamiana* leaves co-expressing TET8-mCherry with *SAG21-3WJ-4xBro*, *APS1-3WJ-4xBro*, *PRXIIC-3WJ-4xBro*, *HEL-3WJ-4xBro*, or *OEP6-3WJ-4xBro*, showing that plant *SAG21-*, *APS1-*, *PRXIIC-*, and *HEL-3WJ-4xBro* tagged mRNAs were observed in EVs, whereas the *OEP6* control was not. Scale bars, 5 μm.

(B) Quantification of tagged transcripts in EVs isolated from *N. benthamiana* in (A). The data are presented as mean ± SD, n = 6 optical slices. Ordinary one-way ANOVA using Dunnett's multiple comparisons test (B, C, E, and F) was conducted to identify statistically significant differences. Small black circles (B, C, E, and F) represent individual values.

(C) Quantification of protein TET8-mCherry in EVs isolated from *N. benthamiana* in (A). The data are presented as mean ± SD, n = 6 optical slices.

(D) Confocal images of EVs isolated from *Arabidopsis* transgenic lines expressing *SAG21-3WJ-4xBro* (line #2), *APS1-3WJ-4xBro* (line #2), or *OEP6-3WJ-4xBro* (line #2) transcripts. Plant *SAG21-* and *APS1-3WJ-4xBro* tagged mRNAs, but not *OEP6-3WJ-4xBro* were detected in EVs. The lipophilic FM4-64 dye was used to stain EVs. Scale bars, 5 μm.

(E) Quantification of tagged transcripts in EVs isolated from *Arabidopsis* transgenic lines in (D). The data are presented as mean ± SD, n = 6 optical slices.

(F) Quantification of total EVs isolated from *Arabidopsis* transgenic lines in (D). The data are presented as mean ± SD, n = 6 optical slices. See also Figure S2.

Please cite this article in press as: Wang et al., Plant mRNAs move into a fungal pathogen via extracellular vesicles to reduce infection, Cell Host & Microbe (2023), https://doi.org/10.1016/j.chom.2023.11.020

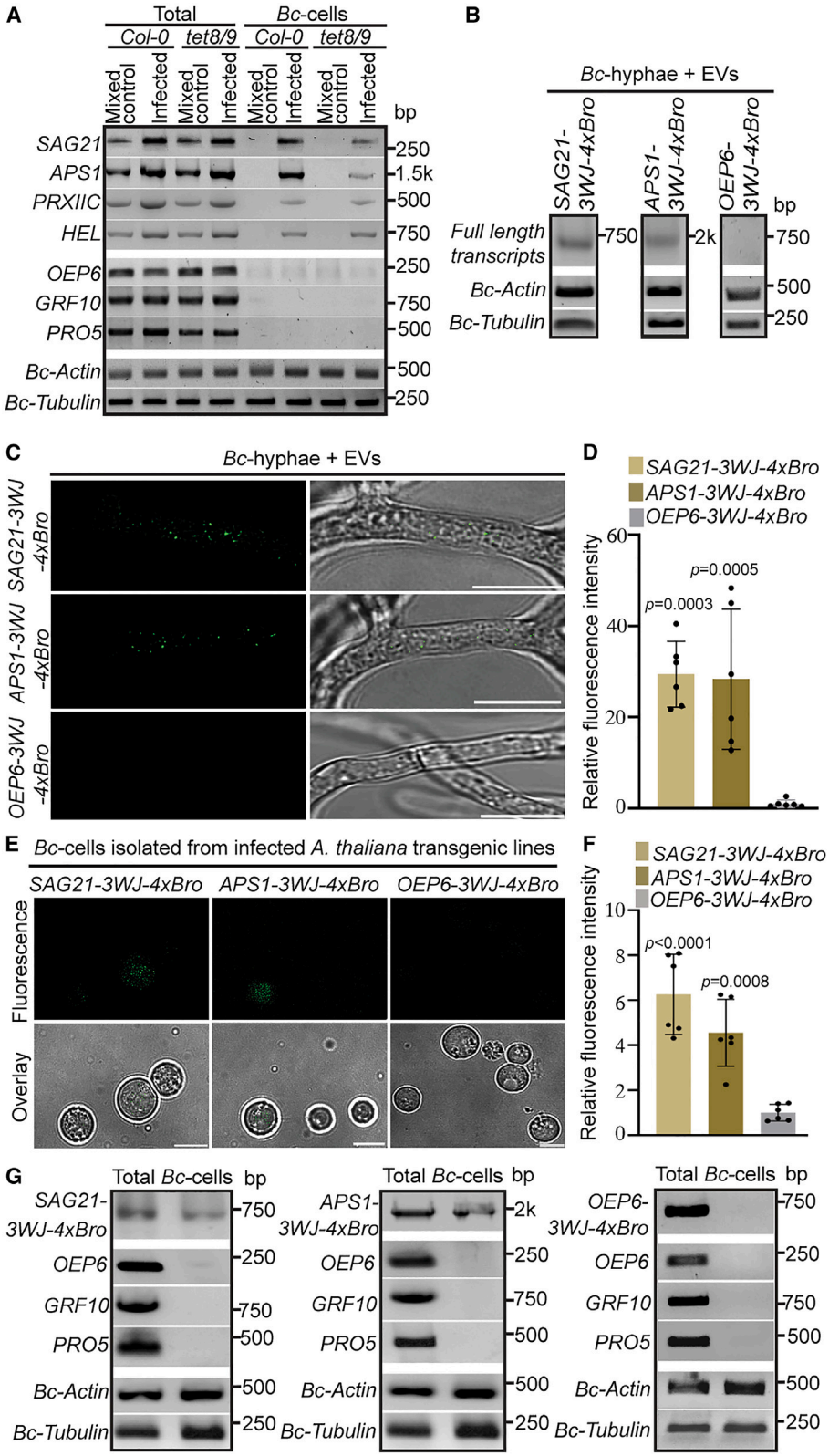

Figure 3. Plant mRNAs are transported into fungal cells

(A) Full-length transcripts were detected by RT-PCR in *B. cinerea* cells isolated from infected *Col-0* (Infected), but not in cultured *B. cinerea* mixed with uninfected leaves (Mixed control), which was subjected to the same procedure. Plant transcripts were reduced in *B. cinerea* cells purified from the infected *tet8*/*tet9* double

(legend continued on next page)

Please cite this article in press as: Wang et al., Plant mRNAs move into a fungal pathogen via extracellular vesicles to reduce infection, Cell Host & Microbe (2023), https://doi.org/10.1016/j.chom.2023.11.020

It remained a possibility that mRNAs were bound to mono-ribosomes and were not actively being translated into proteins. To investigate whether mRNAs were associated with actively translating polysomes, *B. cinerea* cells were isolated from infected *Arabidopsis* leaves, and the cell extracts were then fractionated by sucrose gradient centrifugation to separate the polysomes from monosomes and ribosomal subunits. We focused on *SAG21* and *APS1*, and RT-PCR results showed that these transcripts were highly enriched in fractions containing polysomes, consistent with the *B. cinerea* endogenous control transcript *Bc_Actin* (Figure 4B). To further confirm that *SAG21* and *APS1* accumulated in actively translating polysomes, the fungal cell lysates were treated with the translation inhibitor puromycin, which can specifically disrupt polysomes,[49,50] before being loaded onto sucrose gradients. Like *Bc-Actin*, both *SAG21* and *APS1* plant mRNAs shifted to the more slowly sedimenting monosomal fractions of the gradient (Figure 4B). This result indicates that transferred plant mRNAs are associated with actively translating fungal polysomes and thus are translated into proteins within fungal cells.

To determine whether we can detect the proteins translated from the transferred mRNAs in the fungal cells, we generated *Arabidopsis* transgenic plants in the corresponding mutant background expressing *SAG21-YFP*, *APS1-YFP*, or mutated (*m*) *SAG21-YFP* and *mAPS1-YFP* that could not be translated (Figures S3C–S3E). A premature stop codon was introduced by a single-nucleotide insertion (for *mSAG21*) or replacement (for *mAPS1*) to minimize the change in the mRNA secondary or tertiary structures, which could be required for EV-loading and trafficking. Initially, we tested whether the SAG21-YFP and APS1-YFP proteins are secreted. Immunoblotting showed that both fusion proteins were not detectable in the apoplastic fluid, the P100 EV fraction, or the supernatant of the P100 fraction (Figure 4C). Moreover, SAG21-YFP or APS1-YFP fusion proteins were not detected in TET8-positive EVs when co-expressed with TET8-mCherry in *N. benthamiana* cells (Figures S4A–S4C), whereas the positive control Annexin 1 (ANN1)-YFP fusion was detectable in EVs, which is consistent with a previous report[15] (Figures S4A–S4C). This result demonstrates that the SAG21-YFP and APS1-YFP fusion proteins are not secreted or exported via EVs. Therefore, the presence of SAG21-YFP and APS1-YFP in fungal cells is due to translation of plant mRNAs by fungal ribosomes.

To determine that transferred plant mRNAs are indeed translated in fungal cells, we isolated EVs from uninfected *Arabidopsis* transgenic lines expressing *SAG21-YFP* and *APS1-YFP*. The purified plant EVs, which did not show any detectable fusion proteins (Figures 4C and 4D–4G at 0 h), were incubated with cultured *B. cinerea* conidia for 24 h. Although all the transcripts of *SAG21-YFP*, *APS1-YFP*, *mSAG21-YFP*, and *mAPS1-YFP* were detected in the fungal cells after incubation with isolated EVs for 24 h (Figure 4F), only the fluorescent proteins SAG21-YFP and APS1-YFP from corresponding transgenic *Arabidopsis* lines, but not the mutated versions, were observed in fungal cells incubated with EVs after 24 h (Figures 4D, 4E, and 4G). This provides strong evidence that these proteins were translated from the transferred mRNAs in the fungal cells.

Plant mRNAs in fungal cells reduce infection

To assess if transferred plant mRNAs could act in fungal cells to affect infection, we generated *B. cinerea* transformants that ectopically express *SAG21-YFP, APS1-YFP*, or *mSAG21-YFP*, *mAPS1-YFP*, or free *YFP* as controls. Both *SAG21-YFP* and *APS1-YFP* strains displayed reduced fungal growth compared with *mSAG21-YFP*, *mAPS1-YFP*, or free *YFP* strains (Figure S5A). Both transcripts and proteins were detected in the corresponding *SAG21-YFP* and *APS1-YFP* strains, but only the transcript, not the protein, could be detected in the corresponding *mSAG21-YFP* or *mAPS1-YFP* strains (Figures S5B and S5C). The transformants expressing *SAG21-YFP* or *APS1-YFP* showed significantly reduced infection on *Arabidopsis* compared with the control free *YFP* strain, whereas the *mSAG21-YFP* or *mAPS1-YFP* strain did not show significant differences in terms of infection compared with the free *YFP* strain (Figures 5A and 5B). These results confirm that these transferred mRNAs can limit pathogen infection following translation into proteins. Furthermore, both SAG21-YFP and APS1-YFP proteins partially localized to *Botrytis* mitochondria and resulted in similar morphological changes, with enlarged separated mitochondria and disrupted mitochondrial network (Figure 5C). The free YFP control localized in the cytoplasm and did not alter mitochondrial morphology or network. The morphology change of the mitochondria likely disrupts mitochondrial function and perturbs the subcellular network formed between fungal mitochondria.

mutant line compared with those from infected *Col-0*. *OEP6*, *GRF10*, and *PRO5* were used as plant endogenous controls and *Bc-actin* and *Bc-tubulin* as pathogen controls (A, B, and G). DNA size markers are in base pair (bp) (A, B, and G).

(B) The *Arabidopsis SAG21-3WJ-4xBro* and *APS1-3WJ-4xBro*-tagged transcripts were detected within *B. cinerea* hyphae after co-incubation, whereas OEP6-3WJ-4xBro was not. EVs purified from *Arabidopsis* expressing SAG21-3WJ-4xBro, APS1-3WJ-4xBro, or OEP6-3WJ-4xBro were incubated with *in vitro* cultured *B. cinerea* conidia for 4 h. Tagged transcripts were detected by RT-PCR after Triton-X100 treatment and washing to remove EVs in the mixed solution.

(C) Confocal microscopy shows that fluorescence of tagged transcripts *SAG21-3WJ-4xBro*, *APS1-3WJ-4xBro*, but not *OEP6-3WJ-4xBro*, was observed in *B. cinerea* hyphae after 4 h incubation with EVs expressing corresponding tagged transcripts, which were isolated from the corresponding transgenic plants. *B. cinerea* hyphae was imagined after Triton-X100 treatment and washing to remove EVs outside of the fungal hyphae. Scale bars, 5 μm.

(D) Quantification of plant tagged transcripts in *Botrytis* hyphae in (C). Ordinary one-way ANOVA using Dunnett's multiple comparisons test (D and F) was conducted to identify statistically significant differences. The data are presented as mean ± SD, n = 6 optical slices. Small black circles (D and F) represent individual values.

(E) Confocal images of *B. cinerea* cells isolated from infected transgenic *A. thaliana* lines expressing *SAG21-3WJ-4xBro*, *APS1-3WJ-4xBro*, or *OEP6-3WJ-4xBro* (control) show that plant tagged mRNAs were detected in interacting fungal cells. Scale bars, 5 μm.

(F) Quantification of tagged transcripts in *Botrytis* cells isolated from infected *Arabidopsis* transgenic lines in (E). The data are presented as mean ± SD, n = 6 optical slices.

(G) RT-PCR shows that tagged transcripts translocated from the plants into interacting fungal cells were detected in purified *Bc*-cells. *B. cinerea* cells were isolated from infected transgenic *A. thaliana* lines expressing *SAG21-3WJ-4xBro*, *APS1-3WJ-4xBro*, or *OEP6-3WJ-4xBro* (control).

Please cite this article in press as: Wang et al., Plant mRNAs move into a fungal pathogen via extracellular vesicles to reduce infection, Cell Host & Microbe (2023), https://doi.org/10.1016/j.chom.2023.11.020

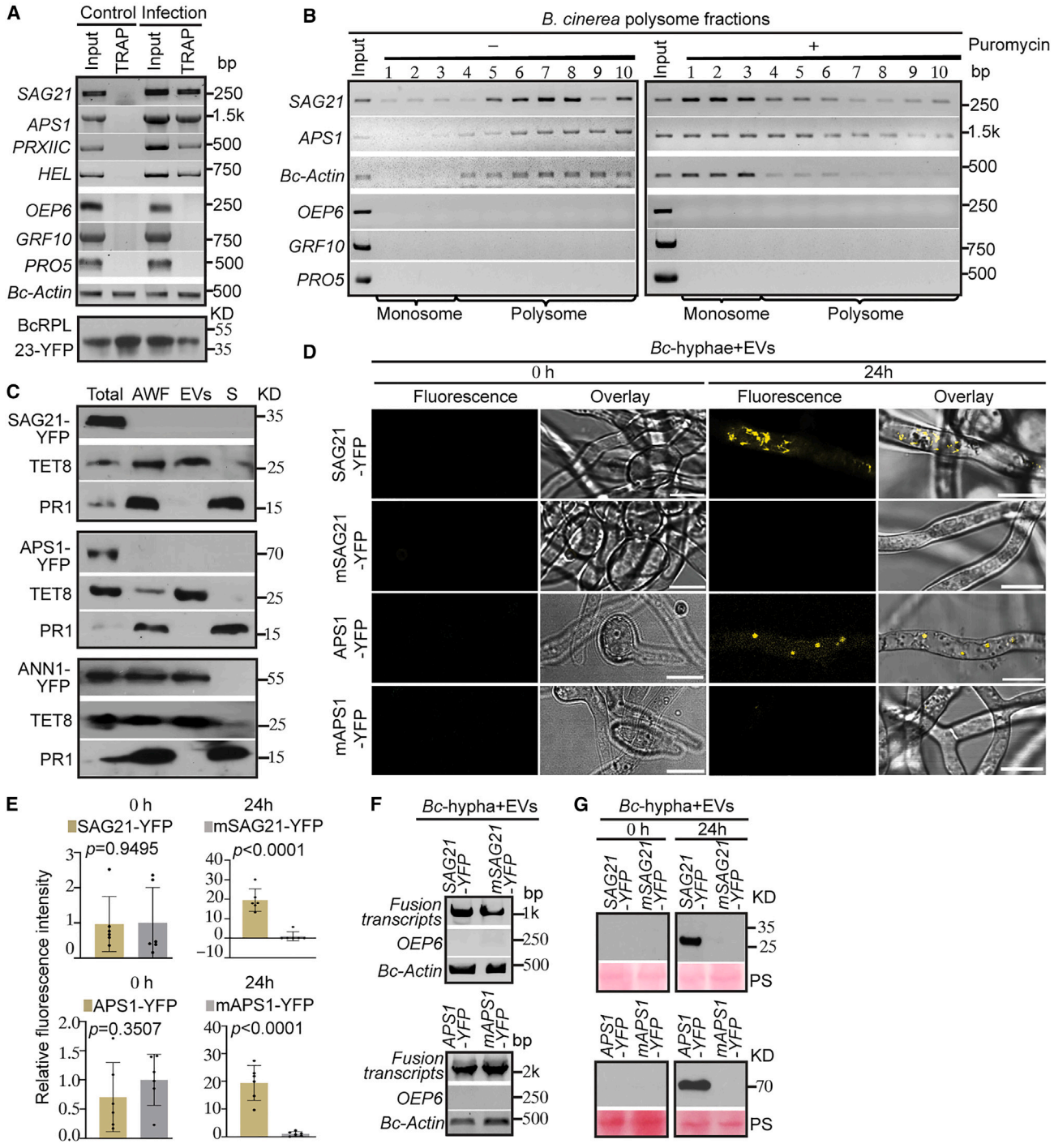

Figure 4. Plant mRNAs are translated in fungal cells

(A) Full-length plant transcripts were detected in TRAP-isolated fungal ribosome fraction after 36 h infection (Infection) by *B. cinerea* expressing ribosomal subunit BcRPL23-YFP, but were not detected in *in vitro* cultured *B. cinerea* transgenic BcRPL23-YFP hyphae mixed with *Col-0* (Control) (upper panels). Immunoblot shows that TRAP specifically pulls down BcRPL23-YFP from infected *Col-0* tissue using α-GFP antibody beads. *OEP6*, *GRF10*, and *PRO5* were used as plant control genes, *Bc-actin* as a pathogen control gene. DNA size markers are in base pair (bp) (A, B, and F). Protein size markers are in kilodaltons (KD) (A and F).

(B) RT-PCR shows that the transferred *Arabidopsis* mRNAs were associated with *B. cinerea* polysomes. The transferred plant mRNAs were shifted from the polysome fractions to the monosome fractions upon puromycin treatment. Ten fractions of equal volume were collected from top to bottom of 15% to 55% sucrose gradients. Treatment of puromycin or not is as indicated (+ or −).

(C) Western blot analysis shows SAG21-YFP and APS1-YFP proteins were not detectable in the extracellular fractions, including apoplastic wash fluids (AWFs), the P100 EV fraction (EVs), or the supernatant of the P100 fraction (S). As a positive control, annexin1(ANN1)-YFP-tagged protein was secreted into AWFs and

(legend continued on next page)

Finally, we also identified T-DNA insertion knockout *Arabidopsis* mutants for *SAG21* and *APS1* (Figures S5D–S5F) and subjected them to *B. cinerea* infection. The mutant lines showed increased susceptibility to *B. cinerea* infection compared with wild-type plants (Figures 5D and 5E), whereas no significant difference was observed between the complemented transgenic lines and wild-type plants (Figures 5D and 5E). These data suggest that *SAG21* and *APS1* contribute to reduced plant susceptibility to fungal infection.

DISCUSSION

Cross-kingdom sRNA trafficking has been observed in a wide range of host-microbe/parasite interaction systems, including both plant and animal hosts with their pathogenic or beneficial microbes.[1,5,6,9–11,37,51,52] Recently, it has been shown that EVs play a role in DNA horizontal gene transfer between bacteria in marine environments, which is mediated by forms of transposons called Tycheposons. Tycheposons are enriched in EVs in seawater, demonstrating that EVs are more stable in a harsh environment than anticipated, and nucleic acid transfer occurs via EVs to accelerate microbial evolution.[53] In this study, we show that specific plant host mRNAs can also be transferred via EVs into an interacting fungal pathogen. EVs provide excellent protection to vulnerable RNA and DNA cargoes during transportation. The presence of the majority of these mRNAs also in EVs from uninfected *Arabidopsis* plants (Figure 1A; Tables S1 and S2) indicates that they are not formed by the necrotizing activities of *B. cinerea* that are observed usually after 48 h of infection on *Arabidopsis* under our infection conditions. Indeed, EVs prepared from uninfected transgenic *Arabidopsis* expressing *3WJ-4xBro*-tagged mRNAs (Figure 3C) allowed us to monitor the transport of those mRNA fusions into fungal cells during co-incubation. These transferred host mRNAs can be translated into proteins in the fungal cells (Figure 4) and have the potential to attenuate infection (Figure 5). Cross-kingdom trafficking of mRNAs is likely to be more effective than trafficking of proteins for modulating microbial infection, due to the ability of mRNAs to be translated into many protein molecules inside the interacting microbial cells, thus amplifying the functional consequences.

The presence of mRNAs in EVs isolated from uninfected plants indicates that EV-mediated mRNA transport may serve as a general mechanism for mRNA transport between different cells or tissues within a plant. Similar phenomena were observed in mammalian systems, where EVs carrying sRNAs and mRNAs move between tissues and cells.[23,24] EVs do not only offer protection of the RNA cargoes from degradation in the extracellular environment but may also facilitate the process of entering the recipient cells or organisms. Transport of existing mRNAs directly between cells and tissues within plants or between plants and interacting organisms may contribute to the rapid host response to environmental stresses or pathogen attacks.

The sequencing profiles of EV-associated mRNAs, as distinct from the total mRNA profiles, suggest selective loading of RNA cargo into EVs (Tables S1 and S3). In mammalian cells, microRNAs carrying 4–7 nucleotides of comprising EXOmotifs, predominantly with high GC content, show significant enrichment in small EVs. Moreover, these EXOmotifs can enhance both small EV secretion and the ability of secreted microRNAs to inhibit target genes in recipient cells.[54] In plants, we have identified a set of EV-associated RNA-binding proteins, including AGO1 and RNA helicases, which contribute to selective sRNA loading into EVs.[15] In this study, we identified a subset of functional mRNAs in plant EVs that can move into interacting fungal cells. Further investigation is necessary to unravel the mechanisms involved in host mRNA selection, packaging, transport, and uptake into interacting fungal cells.

Strikingly, more than 20% of the plant mRNAs that are transported into fungal cells by EVs encode predicted mitochondria-targeted proteins or possess dual-targeting signals for mitochondria and chloroplasts. Our results show, using SAG21 and APS1 proteins, that they have the potential to target fungal mitochondria. Mitochondria are essential organelles in most eukaryotes that produce energy in the form of ATP to enable many cellular processes. They also play a pivotal role in plant and animal immune responses against pathogen infection.[55,56] In both animal and plant fungal pathogens, the importance of mitochondria in fungal pathogenicity has been recognized.[57–60] Although plant mitochondria have been proposed as targets of pathogen effector proteins,[61–63] this study shows that plants have also evolved an analogous strategy to deliver a range of mRNAs that encode proteins that could act synergistically to potentially target and perturb fungal mitochondrial activities. This may occur not through retaining their known functions within plant cells. Rather, we hypothesize that their presence in fungal mitochondria may in some way be detrimental to the fungus, potentially through antagonizing the efficient function of endogenous mitochondrial processes. Future investigation of the biological functions of the proteins encoded by these transferred host mRNAs will help us to understand the importance of

present in EVs. The abundantly secreted pathogen-related protein1 (PR1), absent in EVs, was used as a secretion control. TET8 native protein was used as a marker for EV containing fractions. S, supernatant after 100,000 × *g* centrifugation.

(D) The fluorescence signals of YFP-tagged SAG21 and APS1 proteins were observed in fungal cells only after incubation with EVs isolated from transgenic plants expressing SAG21-YFP or APS1-YFP for 24 h but not at 0 h. There was no fluorescence signal for mSAG21-YFP or mAPS1-YFP after co-incubation. EVs were isolated from corresponding *Arabidopsis* transgenic lines expressing *SAG21-YFP*, *APS1-YFP*, *mSAG21-YFP*, or *mAPS1-YFP*. Scale bars, 10 μm.

(E) Quantification of translated proteins from transferred plant *YFP*-tagged transcripts in fungal hyphae in (D). T test was conducted to identify statistically significant differences. The data are presented as mean ± SD, n = 6 optical slices. Small black circles represent individual values.

(F) RT-PCR shows that the full-length *YFP*-tagged wild-type transcripts *SAG21* and *APS1*, as well as the *YFP*-tagged mutated transcripts *mSAG21* and *mAPS1* were detected in fungal cells incubated with EVs for 24 h (left panels).

(G) Only the transferred wild-type *SAG21* and *APS1* mRNAs but not the mutated versions were translated into tagged proteins in fungal cells. Samples from (D) were subjected to immunoblot using α-GFP as primary antibody (right panels). Size markers are indicated in KD, and protein loading is represented by Ponceau staining (PS).

See also Figures S3 and S4, and Table S4.

Please cite this article in press as: Wang et al., Plant mRNAs move into a fungal pathogen via extracellular vesicles to reduce infection, Cell Host & Microbe (2023), https://doi.org/10.1016/j.chom.2023.11.020

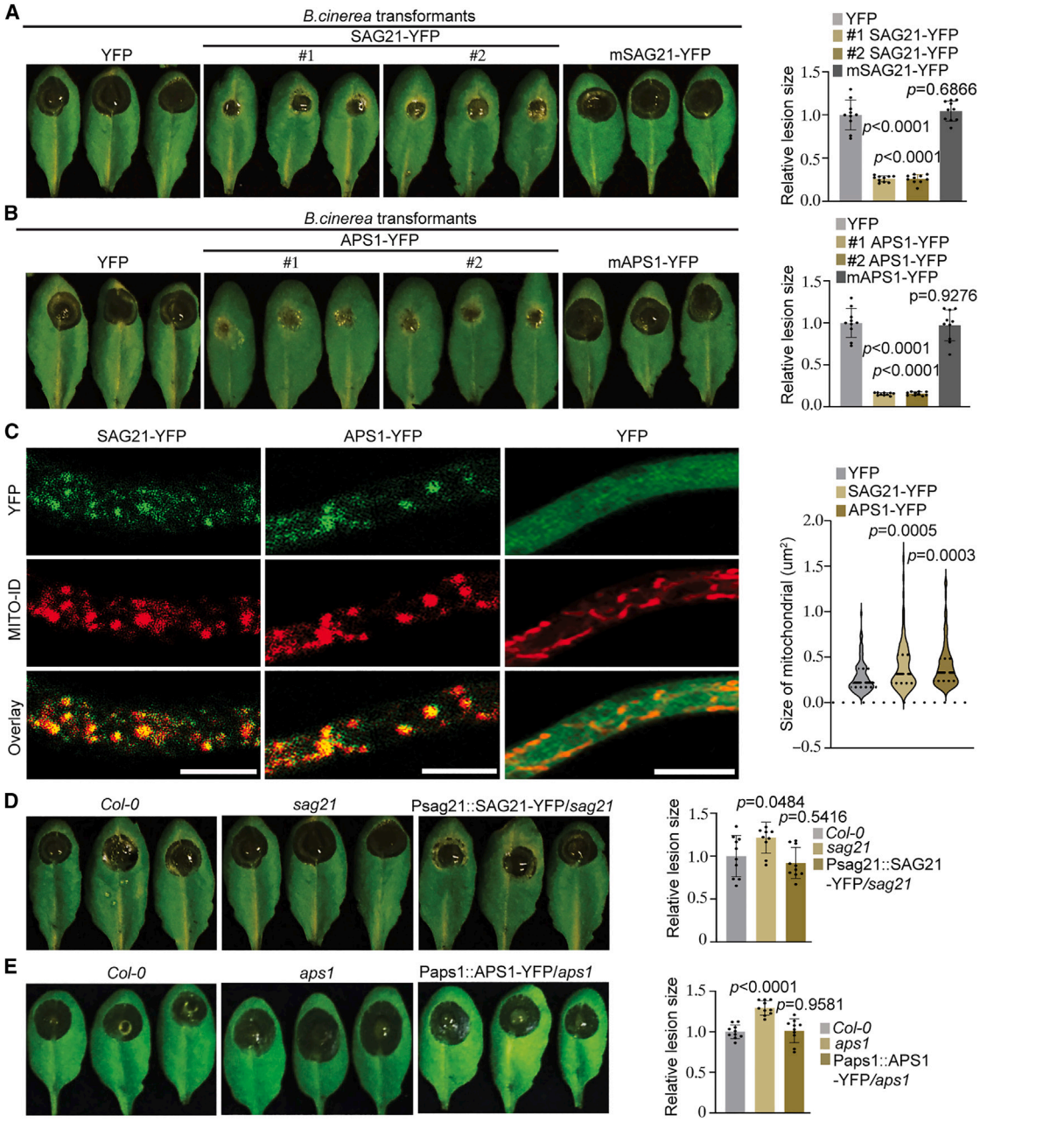

Figure 5. Plant mRNAs in fungal cells reduce infection

(A) *B. cinerea* transformants expressing *Arabidopsis* SAG21-YFP under a constitutive promotor *oliC* in an intergenic region show reduced virulence compared with transformants expressing the mutated transcript mSAG21-YFP or control YFP.

(B) *B. cinerea* transformants expressing APS1-YFP display reduced infection capability compared with transformants expressing mAPS1-YFP or control YFP. For A and B, relative lesion sizes were measured at 60 h post-infection. The data are presented as mean ± SD, n = 10 leaves from at least three replicates. Ordinary one-way ANOVA using Dunnett's multiple comparisons test was conducted to identify statistically significant differences. Small black circles represent individual values.

(C) SAG21-YFP and APS1-YFP, but not the free YFP, are localized in mitochondria in *B. cinerea* transformants ectopically expressing these tagged proteins. Ordinary one-way ANOVA using Dunnett's multiple comparisons test was conducted to identify statistically significant differences. Quantification of mitochondrial morphology change is displayed in violin plots, The size of mitochondrial (n = 100) in *B. cinerea* transformants was measured using Image J. Scale bars, 5 μm.

(D) Enhanced susceptibility to *B. cinerea* was observed in T-DNA insertion knockout line *sag21* (SALK_099663). Complemented transgenic *sag21* line expressing SAG21-YFP driven by its native promotor shows no significant difference in susceptibility with *Col-0*.

(legend continued on next page)

mitochondria in plant-pathogen interactions and precisely how mRNAs such as *SAG21* and *APS1* may modulate fungal mitochondrial morphology and functions.

Our understanding of the mechanisms underlying cross-kingdom RNA trafficking will help in the development of effective and eco-friendly strategies to control plant diseases. With growing evidence to support the capabilities of EVs as attractive molecular vehicles, the discovery of EVs as vehicles to transfer plant RNAs, including sRNAs and mRNAs, into fungal cells will no doubt aid in the development of plant protection solutions.

STAR★METHODS

Detailed methods are provided in the online version of this paper and include the following:

- KEY RESOURCES TABLE
- RESOURCE AVAILABILITY
  - Lead contact
  - Materials availability
  - Data and code availability
- EXPERIMENTAL MODEL AND SUBJECT DETAILS
  - *Arabidopsis thaliana*
  - *Nicotiana benthamiana*
  - *Botrytis Cinerea*
- METHOD DETAILS
  - *Agrobacterium*-mediated transformation
  - Trypan blue stains of *A. thaliana* leaves infected by *B. cinerea*
  - Pathogenesis assay
  - Fungal cell isolation from infected *A. thaliana*
  - Vector construction and transgenic plants
  - *B. cinerea* transformation vector construction and transformation
  - Translating Ribosome Affinity Purification (TRAP) and puromycin treatment
  - Immuno-isolation of EVs
  - Immunoprecipitation and immunoblotting assays
  - Nuclease and proteinase K protection assay
  - RT-PCR and gene expression analyses
  - Confocal microscopy
  - Transmission electron microscopy (TEM)
  - Nanoparticle Tracking Analysis (NTA)
  - Assay to measure transcript delivery and translation from EVs
  - *B. cinerea in vitro* growth assay
  - RNA-seq and data analysis
- QUANTIFICATION AND STATISTICAL ANALYSIS

SUPPLEMENTAL INFORMATION

Supplemental information can be found online at https://doi.org/10.1016/j.chom.2023.11.020.

ACKNOWLEDGMENTS

We thank Prof. Julia Bailey-Serres for helpful advice on TRAP and polysome analysis, as well as for sharing ultracentrifuge to isolate *B. cinerea* polysome fractions. We thank Dr. Angela Chen for assisting with the nanoparticle assay and Yifan Huang for TEM of EVs. This work was supported by grants from the National Institute of Health (R35GM136379), the National Science Foundation (IOS 2020731), and United State Department of Agriculture (2021-67013-34258) to H.J.; National Natural Science Foundation of China (32272029, 32070288) and Hubei Provincial Natural Science Foundation of China (2022CFA079) to Q.C.; ERC Advanced grant PathEVome (787764) to P.B.

AUTHOR CONTRIBUTIONS

H.J. conceived the idea and supervised the project. H.J., S.W., and P.B. designed the experiments. S.W. performed most of the experiments and analyzed data. B.H. performed polysome analysis and helped in making some constructs and *Botrytis* transformation; Q.C. performed mRNA-seq of EVs. H.W. helped in making constructs and genotyping. C.A.-G. and O.R.-S. conducted RNA-seq data analysis. S.W., H.J., and P.B. wrote the manuscript, and all authors contributed to revision.

DECLARATION OF INTERESTS

The authors declare no competing interests.

Received: July 27, 2023
Revised: October 17, 2023
Accepted: November 20, 2023
Published: December 15, 2024

REFERENCES

1. Cai, Q., He, B., Wang, S., Fletcher, S., Niu, D., Mitter, N., Birch, P.R.J., and Jin, H. (2021). Message in a bubble: shuttling small RNAs and proteins between cells and interacting organisms using extracellular vesicles. Annu. Rev. Plant Biol. *72*, 497–524.
2. Bielska, E., and May, R.C. (2019). Extracellular vesicles of human pathogenic fungi. Curr. Opin. Microbiol. *52*, 90–99.
3. Olive, A.J., and Sassetti, C.M. (2016). Metabolic crosstalk between host and pathogen: sensing, adapting and competing. Nat. Rev. Microbiol. *14*, 221–234.
4. Baulcombe, D. (2004). RNA silencing in plants. Nature *431*, 356–363.
5. Weiberg, A., Wang, M., Lin, F.M., Zhao, H., Zhang, Z., Kaloshian, I., Huang, H.D., and Jin, H. (2013). Fungal small RNAs suppress plant immunity by hijacking host RNA interference pathways. Science *342*, 118–123.
6. Chen, A., Halilovic, L., Shay, J.H., Koch, A., Mitter, N., and Jin, H. (2023). Improving RNA-based crop protection through nanotechnology and insights from cross-kingdom RNA trafficking. Curr. Opin. Plant Biol. *76*, 102441.
7. Dunker, F., Trutzenberg, A., Rothenpieler, J.S., Kuhn, S., Prols, R., Schreiber, T., Tissier, A., Kemen, A., Kemen, E., Huckelhoven, R., et al. (2020). Oomycete small RNAs bind to the plant RNA-induced silencing complex for virulence. Elife *9*, e56096.
8. Cui, C., Wang, Y., Liu, J., Zhao, J., Sun, P., and Wang, S. (2019). A fungal pathogen deploys a small silencing RNA that attenuates mosquito immunity and facilitates infection. Nat. Commun. *10*, 4298.
9. Ren, B., Wang, X., Duan, J., and Ma, J. (2019). Rhizobial tRNA-derived small RNAs are signal molecules regulating plant nodulation. Science *365*, 919–922.

(E) The *APS1* T-DNA insertion knockout line (*aps1*, SALK_046518) shows enhanced susceptibility to *B. cinerea*. Complemented transgenic *aps1* line expressing APS1-YFP driven by its native promotor shows no significant difference in susceptibility with *Col-0*. For (D and E), relative lesion sizes were measured at 60 h post-infection. The data are presented as mean ± SD, n = 10 leaves from at least three replicates. Ordinary one-way ANOVA using Dunnett's multiple comparisons test was conducted to identify statistically significant differences. Small black circles represent individual values. See also Figure S5.

10. Cai, Q., Qiao, L., Wang, M., He, B., Lin, F.M., Palmquist, J., Huang, S.D., and Jin, H. (2018). Plants send small RNAs in extracellular vesicles to fungal pathogen to silence virulence genes. Science *360*, 1126–1129.

11. Huang, C.Y., Wang, H., Hu, P., Hamby, R., and Jin, H. (2019). Small RNAs - big players in plant-microbe interactions. Cell Host Microbe *26*, 173–182.

12. Halder, L.D., Babych, S., Palme, D.I., Mansouri-Ghahnavieh, E., Ivanov, L., Ashonibare, V., Langenhorst, D., Prusty, B., Rambach, G., Wich, M., et al. (2021). Candida albicans induces cross-kingdom miRNA trafficking in human monocytes to promote fungal growth. mBio *13*, e0356321.

13. Cai, Q., Halilovic, L., Shi, T., Chen, A., He, B., Wu, H., and Jin, H. (2023). Extracellular vesicles: cross-organismal RNA trafficking in plants, microbes, and mammalian cells. Extracell. Vesicles Circ. Nucl. Acids *4*, 262–282.

14. Liu, Y.J., and Wang, C. (2023). A review of the regulatory mechanisms of extracellular vesicles-mediated intercellular communication. Cell Commun. Signal. *21*, 77.

15. He, B., Cai, Q., Qiao, L., Huang, C.Y., Wang, S., Miao, W., Ha, T., Wang, Y., and Jin, H. (2021). RNA-binding proteins contribute to small RNA loading in plant extracellular vesicles. Nat. Plants *7*, 342–352.

16. Valero-Jiménez, C.A., Veloso, J., Staats, M., and van Kan, J.A.L. (2019). Comparative genomics of plant pathogenic Botrytis species with distinct host specificity. BMC Genomics *20*, 203.

17. He, B., Wang, H., Liu, G., Chen, A., Calvo, A., Cai, Q., and Jin, H. (2023). Fungal small RNAs ride in extracellular vesicles to enter plant cells through clathrin-mediated endocytosis. Nat. Commun. *14*, 4383.

18. O'Brien, K., Breyne, K., Ughetto, S., Laurent, L.C., and Breakefield, X.O. (2020). RNA delivery by extracellular vesicles in mammalian cells and its applications. Nat. Rev. Mol. Cell Biol. *21*, 585–606.

19. Maizel, A., Markmann, K., Timmermans, M., and Wachter, A. (2020). To move or not to move: roles and specificity of plant RNA mobility. Curr. Opin. Plant Biol. *57*, 52–60.

20. Kehr, J., Morris, R.J., and Kragler, F. (2022). Long-distance transported RNAs: from identity to function. Annu. Rev. Plant Biol. *73*, 457–474.

21. Kitagawa, M., Tran, T.M., and Jackson, D. (2023). Traveling with purpose: cell-to-cell transport of plant mRNAs. Trends Cell Biol.

22. Temoche-Diaz, M.M., Shurtleff, M.J., Nottingham, R.M., Yao, J., Fadadu, R.P., Lambowitz, A.M., and Schekman, R. (2019). Distinct mechanisms of microRNA sorting into cancer cell-derived extracellular vesicle subtypes. eLife *8*.

23. Yokoi, A., Yoshioka, Y., Yamamoto, Y., Ishikawa, M., Ikeda, S.I., Kato, T., Kiyono, T., Takeshita, F., Kajiyama, H., Kikkawa, F., et al. (2017). Malignant extracellular vesicles carrying MMP1 mRNA facilitate peritoneal dissemination in ovarian cancer. Nat. Commun. *8*, 14470.

24. Valadi, H., Ekström, K., Bossios, A., Sjöstrand, M., Lee, J.J., and Lötvall, J.O. (2007). Exosome-mediated transfer of mRNAs and microRNAs is a novel mechanism of genetic exchange between cells. Nat. Cell Biol. *9*, 654–659.

25. Kwon, S., Rupp, O., Brachmann, A., Blum, C.F., Kraege, A., Goesmann, A., and Feldbrügge, M. (2021). Mrna inventory of extracellular vesicles from Ustilago maydis. J. Fungi (Basel) *7*.

26. Huang, Y., Wang, S., Cai, Q., and Jin, H. (2021). Effective methods for isolation and purification of extracellular vesicles from plants. J. Integr. Plant Biol. *63*, 2020–2030.

27. Veloso, J., and van Kan, J.A.L. (2018). Many shades of grey in Botrytis–host plant interactions. Trends Plant Sci. *23*, 613–622.

28. Chou, M.L., Fitzpatrick, L.M., Tu, S.L., Budziszewski, G., Potter-Lewis, S., Akita, M., Levin, J.Z., Keegstra, K., and Li, H.M. (2003). Tic40, a membrane-anchored co-chaperone homolog in the chloroplast protein translocon. EMBO J. *22*, 2970–2980.

29. Geissler, A., Chacinska, A., Truscott, K.N., Wiedemann, N., Brandner, K., Sickmann, A., Meyer, H.E., Meisinger, C., Pfanner, N., and Rehling, P. (2002). The mitochondrial presequence translocase: an essential role of Tim50 in directing preproteins to the import channel. Cell *111*, 507–518.

30. Mondragon-Palomino, M., and Gaut, B.S. (2005). Gene conversion and the evolution of three leucine-rich repeat gene families in Arabidopsis thaliana. Mol. Biol. Evol. *22*, 2444–2456.

31. Hooper, C.M., Castleden, I.R., Tanz, S.K., Aryamanesh, N., and Millar, A.H. (2017). SUBA4: the interactive data analysis centre for Arabidopsis subcellular protein locations. Nucleic Acids Res. *45*, D1064–D1074.

32. Salleh, F.M., Evans, K., Goodall, B., Machin, H., Mowla, S.B., Mur, L.A., Runions, J., Theodoulou, F.L., Foyer, C.H., and Rogers, H.J. (2012). A novel function for a redox-related LEA protein (SAG21/AtLEA5) in root development and biotic stress responses. Plant Cell Environ. *35*, 418–429.

33. Traynor, A.M., Sheridan, K.J., Jones, G.W., Calera, J.A., and Doyle, S. (2019). Involvement of sulfur in the biosynthesis of essential metabolites in pathogenic fungi of animals, particularly Aspergillus spp.: molecular and therapeutic implications. Front. Microbiol. *10*, 2859.

34. Anjum, N.A., Gill, R., Kaushik, M., Hasanuzzaman, M., Pereira, E., Ahmad, I., Tuteja, N., and Gill, S.S. (2015). ATP-sulfurylase, sulfur-compounds, and plant stress tolerance. Front. Plant Sci. *6*, 210.

35. Perkins, A., Nelson, K.J., Parsonage, D., Poole, L.B., and Karplus, P.A. (2015). Peroxiredoxins: guardians against oxidative stress and modulators of peroxide signaling. Trends Biochem. Sci. *40*, 435–445.

36. Bertini, L., Proietti, S., Aleandri, M.P., Mondello, F., Sandini, S., Caporale, C., and Caruso, C. (2012). Modular structure of HEL protein from *Arabidopsis* reveals new potential functions for PR-4 proteins. Biol. Chem. *393*, 1533–1546.

37. Cai, Q., He, B., Weiberg, A., Buck, A.H., and Jin, H. (2019). Small RNAs and extracellular vesicles: new mechanisms of cross-species communication and innovative tools for disease control. PLoS Pathog. *15*, e1008090.

38. He, B., Hamby, R., and Jin, H. (2021). Plant extracellular vesicles: Trojan horses of cross-kingdom warfare. FASEB Bioadv. *3*, 657–664.

39. Liu, N.J., Wang, N., Bao, J.J., Zhu, H.X., Wang, L.J., and Chen, X.Y. (2020). Lipidomic analysis reveals the importance of GIPCs in Arabidopsis Leaf extracellular vesicles. Mol. Plant *13*, 1523–1532.

40. Bai, J., Luo, Y., Wang, X., Li, S., Luo, M., Yin, M., Zuo, Y., Li, G., Yao, J., Yang, H., et al. (2020). A protein-independent fluorescent RNA aptamer reporter system for plant genetic engineering. Nat. Commun. *11*, 3847.

41. Filonov, G.S., Moon, J.D., Svensen, N., and Jaffrey, S.R. (2014). Broccoli: rapid selection of an RNA mimic of green fluorescent protein by fluorescence-based selection and directed evolution. J. Am. Chem. Soc. *136*, 16299–16308.

42. Ge, C., Spånning, E., Glaser, E., and Wieslander, A. (2014). Import determinants of organelle-specific and dual targeting peptides of mitochondria and chloroplasts in Arabidopsis thaliana. Mol. Plant *7*, 121–136.

43. Klepikova, A.V., Kasianov, A.S., Gerasimov, E.S., Logacheva, M.D., and Penin, A.A. (2016). A high resolution map of the Arabidopsis thaliana developmental transcriptome based on RNA-seq profiling. Plant J. *88*, 1058–1070.

44. Buxdorf, K., Yaffe, H., Barda, O., and Levy, M. (2013). The effects of glucosinolates and their breakdown products on necrotrophic fungi. PLoS One *8*, e70771.

45. Cai, Q., and Jin, H. (2021). Small RNA extraction and quantification of isolated fungal cells from plant tissue by the sequential Protoplastation. Methods Mol. Biol. *2170*, 219–229.

46. Reynoso, M.A., Kajala, K., Bajic, M., West, D.A., Pauluzzi, G., Yao, A.I., Hatch, K., Zumstein, K., Woodhouse, M., Rodriguez-Medina, J., et al. (2019). Evolutionary flexibility in flooding response circuitry in angiosperms. Science *365*, 1291–1295.

47. Zanetti, M.E., Chang, I.F., Gong, F., Galbraith, D.W., and Bailey-Serres, J. (2005). Immunopurification of polyribosomal complexes of Arabidopsis for global analysis of gene expression. Plant Physiol. *138*, 624–635.

48. Shen, L., Su, Z., Yang, K., Wu, C., Becker, T., Bell-Pedersen, D., Zhang, J., and Sachs, M.S. (2021). Structure of the translating Neurospora ribosome arrested by cycloheximide. Proc. Natl. Acad. Sci. USA. *118*.

49. Chassé, H., Boulben, S., Costache, V., Cormier, P., and Morales, J. (2017). Analysis of translation using polysome profiling. Nucleic Acids Res. *45*, e15.

50. Wang, Y., Li, S., Zhao, Y., You, C., Le, B., Gong, Z., Mo, B., Xia, Y., and Chen, X. (2019). NAD+-capped RNAs are widespread in the Arabidopsis transcriptome and can probably be translated. Proc. Natl. Acad. Sci. USA. *116*, 12094–12102.

51. Liu, S., da Cunha, A.P., Rezende, R.M., Cialic, R., Wei, Z., Bry, L., Comstock, L.E., Gandhi, R., and Weiner, H.L. (2016). The host shapes the gut microbiota via fecal microRNA. Cell Host Microbe *19*, 32–43.

52. Wong-Bajracharya, J., Singan, V.R., Monti, R., Plett, K.L., Ng, V., Grigoriev, I.V., martin, F.M., Anderson, I.C., and Plett, J.M. (2022). The ectomycorrhizal fungus Pisolithus microcarpus encodes a microRNA involved in cross-kingdom gene silencing during symbiosis. Proc Natl Acad. Sci. USA. 119. https://doi.org/10.1073/pnas.2103527119.

53. Hackl, T., Laurenceau, R., Ankenbrand, M.J., Bliem, C., Cariani, Z., Thomas, E., Dooley, K.D., Arellano, A.A., Hogle, S.L., Berube, P., et al. (2023). Novel integrative elements and genomic plasticity in ocean ecosystems. Cell *186*, 47–62.e16.

54. Garcia-Martin, R., Wang, G., Brandão, B.B., Zanotto, T.M., Shah, S., Kumar Patel, S., Schilling, B., and Kahn, C.R. (2022). MicroRNA sequence codes for small extracellular vesicle release and cellular retention. Nature *601*, 446–451.

55. Wang, J., Xu, G., Ning, Y., Wang, X., and Wang, G.L. (2022). Mitochondrial functions in plant immunity. Trends Plant Sci. *27*, 1063–1076.

56. Tiku, V., Tan, M.W., and Dikic, I. (2020). Mitochondrial functions in infection and immunity. Trends Cell Biol. *30*, 263–275.

57. Verma, S., Shakya, V.P.S., and Idnurm, A. (2018). Exploring and exploiting the connection between mitochondria and the virulence of human pathogenic fungi. Virulence *9*, 426–446.

58. Khan, I.A., Ning, G., Liu, X., Feng, X., Lin, F., and Lu, J. (2015). Mitochondrial fission protein MoFis1 mediates conidiation and is required for full virulence of the rice blast fungus Magnaporthe oryzae. Microbiol. Res. *178*, 51–58.

59. Lin, Z., Wu, J., Jamieson, P.A., and Zhang, C. (2019). Alternative oxidase is involved in the pathogenicity, development, and oxygen stress response of Botrytis cinerea. Phytopathology *109*, 1679–1688.

60. An, B., Li, B., Li, H., Zhang, Z., Qin, G., and Tian, S. (2016). Aquaporin8 regulates cellular development and reactive oxygen species production, a critical component of virulence in Botrytis cinerea. New Phytol. *209*, 1668–1680.

61. Xu, G., Zhong, X., Shi, Y., Liu, Z., Jiang, N., Liu, J., Ding, B., Li, Z., Kang, H., Ning, Y., et al. (2020). A fungal effector targets a heat shock-dynamin protein complex to modulate mitochondrial dynamics and reduce plant immunity. Sci. Adv. *6*, eabb7719.

62. Han, J., Wang, X., Wang, F., Zhao, Z., Li, G., Zhu, X., Su, J., and Chen, L. (2021). The fungal effector Avr-Pita suppresses innate immunity by increasing COX activity in rice mitochondria. Rice (N Y) *14*, 12.

63. Tzelepis, G., Dölfors, F., Holmquist, L., and Dixelius, C. (2021). Plant mitochondria and chloroplasts are targeted by the Rhizoctonia solani RsCRP1 effector. Biochem. Biophys. Res. Commun. *544*, 86–90.

64. Ewels, P., Magnusson, M., Lundin, S., and Käller, M. (2016). MultiQC: summarize analysis results for multiple tools and samples in a single report. Bioinformatics *32*, 3047–3048.

65. Dobin, A., Davis, C.A., Schlesinger, F., Drenkow, J., Zaleski, C., Jha, S., Batut, P., Chaisson, M., and Gingeras, T.R. (2013). STAR: ultrafast universal RNA-seq aligner. Bioinformatics *29*, 15–21.

66. Liao, Y., Smyth, G.K., and Shi, W. (2019). The R package Rsubread is easier, faster, cheaper and better for alignment and quantification of RNA sequencing reads. Nucleic Acids Res. *47*, e47.

67. Robinson, M.D., McCarthy, D.J., and Smyth, G.K. (2010). edgeR: a Bioconductor package for differential expression analysis of digital gene expression data. Bioinformatics *26*, 139–140.

68. Almagro Armenteros, J.J., Tsirigos, K.D., Sønderby, C.K., Petersen, T.N., Winther, O., Brunak, S., von Heijne, G., and Nielsen, H. (2019). SignalP 5.0 improves signal peptide predictions using deep neural networks. Nat. Biotechnol. *37*, 420–423.

69. Hu, P., Zhao, H., Zhu, P., Xiao, Y., Miao, W., Wang, Y., and Jin, H. (2019). Dual regulation of Arabidopsis AGO2 by arginine methylation. Nat. Commun. *10*, 844.

70. Zhang, X., Henriques, R., Lin, S.S., Niu, Q.W., and Chua, N.H. (2006). Agrobacterium-mediated transformation of Arabidopsis thaliana using the floral dip method. Nat. Protoc. *1*, 641–646.

71. Imanifard, Z., Vandelle, E., and Bellin, D. (2018). Measurement of hypersensitive cell death triggered by avirulent bacterial pathogens in Arabidopsis. In Plant Programmed Cell Death. Methods in Molecular Biology, vol 1743., L. De Gara and V. Locato, eds. (Humana Press), pp. 39–50.

72. Wang, M., Weiberg, A., Lin, F.M., Thomma, B.P., Huang, H.D., and Jin, H. (2016). Bidirectional cross-kingdom RNAi and fungal uptake of external RNAs confer plant protection. Nat. Plants *2*, 16151.

73. Cai, Q., and Jin, H. (2021). Small RNA extraction and quantification of isolated fungal cells from plant tissue by the sequential Protoplastation. In RNA Abundance Analysis. Methods in Molecular Biology, vol 2170., H. Jin and I. Kaloshian, eds. (Humna Press), pp. 219–229.

74. Earley, K.W., Haag, J.R., Pontes, O., Opper, K., Juehne, T., Song, K., and Pikaard, C.S. (2006). Gateway-compatible vectors for plant functional genomics and proteomics. Plant J. *45*, 616–629.

75. Levis, C., Fortini, D., and Brygoo, Y. (1997). Transformation of Botrytis cinerea with the nitrate reductase gene (niaD) shows a high frequency of homologous recombination. Curr. Genet. *32*, 157–162.

76. McLellan, H., Boevink, P.C., Armstrong, M.R., Pritchard, L., Gomez, S., Morales, J., Whisson, S.C., Beynon, J.L., and Birch, P.R. (2013). An RxLR effector from Phytophthora infestans prevents re-localisation of two plant NAC transcription factors from the endoplasmic reticulum to the nucleus. PLoS Pathog. *9*, e1003670.

77. McCarthy, D.J., and Smyth, G.K. (2009). Testing significance relative to a fold-change threshold is a TREAT. Bioinformatics *25*, 765–771.

Please cite this article in press as: Wang et al., Plant mRNAs move into a fungal pathogen via extracellular vesicles to reduce infection, Cell Host & Microbe (2023), https://doi.org/10.1016/j.chom.2023.11.020

STAR★METHODS

KEY RESOURCES TABLE

REAGENT or RESOURCE	SOURCE	IDENTIFIER
Antibodies		
Rabbit polyclonal anti-TET8	Hailing Jin (He et al.[15])	N/A
Mouse monoclonal Anti-GFP	Sigma-Aldrich	Cat#11814460001
Rabbit polyclonal anti-mCherry	Abcam	Ca#ab167453
Rabbit polyclonal anti-PR1	Agrisera	Cat# AS10 687
Rabbit immunoglobin G	Thermo Fisher	Ca# 02-6102
Bacterial and virus strains		
One Shot™ TOP10 Chemically Competent *E. coli*	Thermo Fisher	Cat#C404003
E. coli TET8-mCherry	Hailing Jin (Cai et al.[10])	N/A
E. coli ANN1-mCherry	Hailing Jin (He et al.[15])	N/A
E. coli SAG21-YFP	This paper	N/A
E. coli APS1-YFP	This paper	N/A
E. coli mSAG21-YFP	This paper	N/A
E. coli mAPS1-YFP	This paper	N/A
E. coli SAG21-3WJ-4xBro	This paper	N/A
E. coli APS1-3WJ-4xBro	This paper	N/A
E. coli PRXIIC-3WJ-4xBro	This paper	N/A
E. coli HEL-3WJ-4xBro	This paper	N/A
E. coli OEP6-3WJ-4xBro	This paper	N/A
Biological samples		
Plant Extracellular vesicles	*Arabidopsis thaliana*	N/A
Fungal hyphae	*Botrytis cinerea*	N/A
Nicotiana benthamiana leaves	*Nicotiana benthamiana*	N/A
Chemicals, peptides, and recombinant proteins		
Puromycin	Sigma	CAS#58-58-2
DFHBI-1	Sigma	CAS#1241390-29-3
FM4-64	Thermo Fisher	Cat#T13320
uranyl acetate	LADD	N/A
SAG21-YFP	This paper	N/A
APS1-YFP	This paper	N/A
Critical commercial assays		
NEB Next Poly(A) mRNA Magnetic Isolation Module kit	NEB	#E7490
NEBNext® Ultra™ Directional RNA Library Prep Kit	NEB	#E7420
MITO-ID Membrane potential detection kit	Enzo	EZN-51018
Deposited data		
RNA-seq data	This paper	GEO: GSE197077
Experimental models: Organisms/strains		
Arabidopsis SAG21-YFP	This paper	N/A
Arabidopsis APS1-YFP	This paper	N/A
Arabidopsis mSAG21-YFP	This paper	N/A
Arabidopsis mAPS1-YFP	This paper	N/A
Arabidopsis SAG21-3WJ-4xBro	This paper	N/A
Arabidopsis APS1-3WJ-4xBro	This paper	N/A
Arabidopsis PRXIIC-3WJ-4xBro	This paper	N/A
Arabidopsis HEL-3WJ-4xBro	This paper	N/A

(*Continued on next page*)

Please cite this article in press as: Wang et al., Plant mRNAs move into a fungal pathogen via extracellular vesicles to reduce infection, Cell Host & Microbe (2023), https://doi.org/10.1016/j.chom.2023.11.020

Continued

REAGENT or RESOURCE	SOURCE	IDENTIFIER
Arabidopsis OEP6-3WJ-4xBro	This paper	N/A
Arabidopsis ANN1-mCherry	Hailing Jin (He et al.[15])	N/A
Arabidopsis T-DNA line SALK_099663	TAIR	SALK_099663
Arabidopsis T-DNA line SALK_046518	TAIR	SALK_046518
Botrytis SAG21-YFP	This paper	N/A
Botrytis APS1-YFP	This paper	N/A
Botrytis YFP	This paper	N/A
Botrytis mSAG21-YFP	This paper	N/A
Botrytis mAPS1-YFP	This paper	N/A
Oligonucleotides		
See Table S5 for primers	This paper	N/A
Recombinant DNA		
SAG21-YFP	This paper	N/A
APS1-YFP	This paper	N/A
mSAG21-YFP	This paper	N/A
mAPS1-YFP	This paper	N/A
SAG21-3WJ-4xBro	This paper	N/A
APS1-3WJ-4xBro	This paper	N/A
PRXIIC-3WJ-4xBro	This paper	N/A
HEL-3WJ-4xBro	This paper	N/A
OEP6-3WJ-4xBro	This paper	N/A
ANN1-mCherry	Hailing Jin (He et al.[15])	N/A
Software and algorithms		
Image J	National Institutes of Health	https://imagej.net/ij/
FastQC	Simon Andrews	https://www.bioinformatics.babraham.ac.uk/projects/fastqc/
MultiQC	Ewels et al.[64]	https://multiqc.info/
STAR (v. 2.7.5a)	Dobin et al.[65]	http://star.mit.edu/
Rsubread package	Liao et al.[66]	https://bioconductor.org/packages/release/bioc/html/Rsubread.html
edgeR package in R	Robinson et al.[67]	https://bioconductor.org/packages/release/bioc/html/edgeR.html
signalP (v. 5.0b)	Almagro Armenteros et al.[68]	https://services.healthtech.dtu.dk/services/SignalP-5.0/9-Downloads.php

RESOURCE AVAILABILITY

Lead contact

Further information and requests for resources and reagents should be directed to and will be fulfilled by the lead contact, Hailing Jin (hailingj@ucr.edu).

Materials availability

All requests for resources and reagents should be directed to the lead contact author. This study did not generate new unique reagents.

Data and code availability

- RNA-seq data have been deposited at GEO and are publicly available as of the date of publication. Accession number is listed in the key resources table.
- This paper does not report original code.
- Any additional information required to reanalyze the data reported in this paper is available from the lead contact upon request.

EXPERIMENTAL MODEL AND SUBJECT DETAILS

Arabidopsis thaliana

Arabidopsis thaliana transgenic lines and mutants were derived from *Col-0*. *Arabidopsis* plants were grown in a controlled environment glasshouse at 23°C with 55% humidity and 12 h light/12h dark. Four-week-old plants were used for most experiments in this study.

Nicotiana benthamiana

N. benthamiana plants were grown in a greenhouse at 23°C with 12 h light/12h dark conditions for 4-5 weeks.

Botrytis Cinerea

B. cinerea wild-type stain B05.10 and transformants were cultured on potato dextrose broth with 1.5% Agar (PDA) plates at room temperature for two weeks before collecting spores for experiments.

METHOD DETAILS

Agrobacterium-mediated transformation

All *A. thaliana* lines used were in the Columbia background (*Col-0*). *A. thaliana* and *N. benthamiana* plants were grown in a controlled environment glasshouse at 23°C with 55% humidity and 12 h light d^{-1}.[69] For *Agrobacterium*-mediated transient expression in *N. benthamiana*, *A. tumefaciens* strain GV3101 transformed with expression vectors were grown at 28 °C overnight in Luria–Bertani broth containing selective antibiotics. They were then pelleted by centrifugation and resuspended in infiltration buffer (10mM 2-(N-morpholino) ethanesulfonic acid (MES), 10mM $MgCl_2$ and 200 mM acetosyringone, pH 7.5) to a final concentration at OD600 nm = 0.5 and incubated at room temperature for at least 1 h before infiltration into leaves. After 2 days, the infiltrated leaves were collected for immunoblotting. Six-week-old flowering *A. thaliana* plants were transformed by the floral-dip method.[70] Transgenic lines were selected on 50 μg mL^{-1} of hygromycin-supplemented Murashige and Skoog (MS) (Sigma, St. Louis) agar plates for 10 d. Hygromycin-resistant seedlings were transferred to soil for propagation. BASTA resistant transgenic lines were selected with spray seedlings using 120 mg L^{-1} of BASTA solution.

Trypan blue stains of *A. thaliana* leaves infected by *B. cinerea*

The staining solutions and procedure were based on the protocol provided by Imanifard[71] with the following modifications: infected leaves after 16 hpi were transferred into 15 ml falcon tubes with a lid and covered with diluted trypan blue solution. The tubes were placed in a heated water bath and the staining solution was boiled for one minute. The tissue was left overnight in the staining solution and destained the next day by replacing the staining solution with chloral hydrate solution three times.

Pathogenesis assay

B. cinerea stain B05.10 wild type and transformants were cultured in Malt Extract Agar (MEA) medium. The *B. cinerea* spores were suspended in 1% sabouraud maltose broth buffer and inoculated onto four-week-old *Arabidopsis* middle leaves, with 10 μl droplets of spores (10^5/ml) applied to each leaf.[72] Lesion development was measured at 2 days post inoculation using Adobe Photoshop software.

Fungal cell isolation from infected *A. thaliana*

The pure fungal cells were isolated from *B. cinerea*-infected plants using sequential protoplast isolation methods described previously, which are based on the different components of plant and fungal cell walls.[10,73] The first step involves releasing plant protoplasts from infected plants. After being infected by *B. cinerea* (2 x 10^5/ml) for 36h, plant leaves were collected, rinsed then homogenized for 1 minute in isolation buffer (0.02 M MOPS buffer pH 7.2, 0.2 M sucrose) in a blender to release fungal cells from infected plants. The homogenate was then filtered through 70 μm nylon mesh to remove plant cell wall debris. The material retained on the filter was re-homogenized and re-filtered. After centrifuging the pooled homogenate at 1,500 g for 10 minutes, the pellets were re-suspended in 1% Triton X-100 and washed 3 times with isolation buffer to remove plant contents. The pellets were then processed for plant cell wall digestion using plant cell wall digest solution (1.5% cellulose, 0.4% maceroenzyme, 0.4 M mannitol, 20 mM MES (pH 5.7), 20 mM KCl, CaCl2, 0.1% BSA) for 2 hours to release the plant protoplasts. The plant protoplasts were ruptured in 1% Triton X-100 and washed in isolation buffer 5 times to completely remove plant contents. The second step involves isolating fungal protoplasts from the previous sample pellet by resuspending the pellet in lysing enzyme solution (2% lysing enzyme from Trichoderma harzianum (Sigma) in 0.6 M KCl, 50 mM CaCl2) and incubating it for 2-3 hours at 28°C. The fungal protoplasts were filtered through a 40 μm nylon mesh and isolated by centrifugating in a 30% sucrose cushion at 4°C for 10 minutes at 5,000 rpm. The fungal protoplasts were collected from the interface between the sucrose layer and the tissue suspension layer, then washed with five- to ten-fold volume of SM buffer (1.2 M-sorbitol and 0.02 M-MES, pH 6.0) and centrifuged at 5,000 rpm for 5 minutes. Repeat the sucrose density gradient centrifugation steps to ensure the removal of any contaminants. The purity of isolated fungal cells was validated by both microscopy and PCR amplification of abundant plant genes (*OEP6, GRF10,PRO5*).

Please cite this article in press as: Wang et al., Plant mRNAs move into a fungal pathogen via extracellular vesicles to reduce infection, Cell Host & Microbe (2023), https://doi.org/10.1016/j.chom.2023.11.020

Vector construction and transgenic plants

For assembly of the constructs expressing *Arabidopsis* genes driven by their native promotor, the gene (*SAG21*) 3' untranslated region (UTR) was amplified with gene-specific primers (Table S5) modified to contain restriction enzyme recognition sites to amplify the gene from gDNA of *Col-0*. PCR products were purified and digested with restriction endonucleases and ligated into the same restriction sites in the plasmid *pENTR-YFP* to generate *pENTR-YFP-SAG21-3'UTR*. The YFP had first been introduced into pENTR vector using restriction endonucleases. 1685 bp of the *SAG21* 5' upstream region, containing the native promoter (NP) coupled with the gene protein coding sequence (CDS) region were amplified from gDNA of *Col-0*, PCR products were introduced into *pENTR-YFP-SAG21-3'UTR* plasmid using restriction endonucleases to create *pENTR-NP-SAG21-YFP-3'UTR*, and recombined with pEarleyGate 302 (PEG302)[74] for expression of C-terminal YFP fusion proteins (*pSAG21::5'UTR-SAG21-YFP-3'UTR*). The construct (*pAPS1::5'UTR-APS1-YFP-3'UTR*) for expressing *APS1-YFP* fusion protein driven by its native promotor (1500 bp) was achieved similar to *SAG21-YFP* as described above.

For generating constructs expressing *Arabidopsis* genes driven by 35S promotor, *SAG21* with UTR was amplified as described above and ligated into PENTR-YFP to generate *pENTR-5'UTR-SAG21-YFP-3'UTR*, and recombined with pEarleyGate 100 (PEG100)[74] for expression of C-terminal YFP fusion proteins (*35S::5'UTR-SAG21-YFP-3'UTR*). *Arabidopsis* mutant transcripts (*mSAG21* and *mAPS1*) were generated using overlap PCR, in which a stop code was introduced in position 83aa (*mSAG21*) or 171aa (*mAPS1*). The constructs for expressing APS1-YFP, mSAG21-YFP or mAPS1-YFP driven by 35S promotor were achieved similar to SAG21-YFP as described above.

For generating constructs expressing *Arabidopsis* or *N. benthamiana* C-terminally tagged *3WJ-4xBro* fusion transcripts, *3WJ-4xBro* DNA sequences were artificially synthesized (GeneScript) and cloned into the plasmid *pENTR* using restriction endonucleases digestion to form *pENTR-3WJ-4xBro*. The *Arabidopsis* genes were amplified from cDNA of *Col-0*, with restriction enzyme recognition sites at both termini. PCR products were purified and ligated into *pENTR-3WJ-4xBro*. The entry clones were recombined with PEG100 for expression of C-terminal *3WJ-4xBro* fusion transcripts (*35S::5'UTR-SAG21-3WJ-4xBro-3'UTR*; *35S::5'UTR-APS1-3WJ-4xBro-3'UTR*; *35S::5'UTR-PRXIIC-3WJ-4xBro-3'UTR*; *35S::5'UTR-HEL-3WJ-4xBro-3'UTR*; *35S::5'UTR-OEP6-3WJ-4xBro-3'UTR*;). All constructs were electroporated into *Agrobacterium tumefaciens* strain GV3101 for expression *in planta*.

B. cinerea transformation vector construction and transformation

The entry clones of *Arabidopsis* genes (*SAG2, APS1*, *mSAG21* and *mAPS1*) were recombined with vector *PB-HPH*, driven by the constitutive promotor *oil*C carrying the *Escherichia coli* hygromycin phosphotransferase gene (*hph*) conferring hygromycin B resistance. The specific primers 1-5-S, 1-3-A (Table S5) were used to amplify dsDNA fragments contain promotor *oil*C, inserted genes and *hph* for *B. cinerea* transformation.

Transformation of *B. cinerea* was achieved using a modified homologous recombination protocol as follows.[75] Briefly, young hyphae were collected from overnight culture of *B. cinerea* grown in yeast extract peptone dextrose (YEPD) and washed twice in KCl buffer (0.6 M KCl, 50 mM $CaCl_2$, PH 6). Protoplasts were generated with 2 % (w/v) Lysing Enzymes from *Trichoderma harzianum* (Sigma) in KCl buffer, and incubated for 2-3 h at room temperature with shaking at 80 rpm. The digested solution was filtered using 70 μm cell strainer (Thermo Fisher). Protoplasts were pelleted by centrifugation at 1,000 × *g* for 3 min at 4 °C, washed twice in ice cold KCl buffer and once in STC buffer (800mM Sorbital, 50 mM Tris, 50 mM $CaCl_2$), resuspended in STC buffer to a final concentration of 10^8 protoplasts ml^{-1}, with adding 1/5 volume of 40 % PSTC solution (Polyethylene glycol (PEG) in STC buffer (w/v)) slowly. 30 μg dsDNA were well mixed with 5 mM spermidine and 1mL prepared protoplasts were maintained on ice for 30 mins. 1 mL 40 % PSTC solution was added to the mixture and gently mixed, then incubated for 20 min at room temperature. For protoplast regeneration, the mixture was incubated in 20 mL RM medium (1L contains 1g Yeast extract, 1g Casamino acid, 274g Sucrose, PH 6.5) for 12-16 h at room temperature (RT) with gentle shaking. Protoplasts were mixed with Potato Dextrose Agar (PDA) medium containing 50 μg/ml of hygromycin B and spread on 90 mm plates. After 3 days of incubation at room temperature, regenerated colonies of *B. cinerea* were individually transferred to fresh MEA medium containing 50 μg/ml of hygromycin B for further analysis.

Translating Ribosome Affinity Purification (TRAP) and puromycin treatment

Arabidopsis leaves were infected by *B. cinerea* transformants expressing *BcRPL23-YFP* for 36 h, frozen in liquid nitrogen, and pulverized infected leaf tissue (2 g) was homogenized in 4 mL of polysome extraction buffer (PEB, 200 mM Tris-HCl, pH 7.5, 200 mM KCl, 25 mM EGTA, 36 mM $MgCl_2$, 1% (v/v) Triton X-100, 1% (v/v) Tween 20, 1% (w/v) Brij-35, 1% (v/v) Igepal CA-630, 5 mM dithiothreitol (DTT), 1 mM phenylmethylsulfonyl fluoride (PMSF) ,50 μg mL^{-1} cycloheximide).

All procedures were performed at 4 °C. After clarification by centrifugation at 16,000xg for 15 min, and approximately 8 mL supernatant were incubated with 200μl GFP-Trap® magnetic beads (ChromoTek) at 4 °C for 2 h with gentle shaking. This was followed by washing the beads three times in 1 mL wash buffer (200 mM Tris-HCl, pH 7.5, 200 mM KCl, 25 mM EGTA, 36 mM $MgCl_2$, 5 mM DTT, 50 μg mL^{-1} cycloheximide). The magnetic beads were subjected to RNA extraction with TRIzol (Thermo Fisher) or stored at -80 °C for immunoblotting.

For puromycin treatment, *B. cinerea* cells were isolated from infected plant leaves, fungal cell lysates were prepared in PEB (exclude cycloheximide) as above. The lysates were centrifuged at 12,000 rpm for 5 min at 4°C after incubation on ice for 10 min. Sodium deoxycholate was added to the supernatant at a concentration of 0.5%, and the mixture was then placed on ice for 5 min. The remaining insoluble materials were removed by centrifuging at 12,000 rpm for 15 min at 4°C. Then 1.0 mg/mL Puromycin (Sigma) was added to the half volume of lysates and incubated for 30 min at room temperature, the other half lysates without

Please cite this article in press as: Wang et al., Plant mRNAs move into a fungal pathogen via extracellular vesicles to reduce infection, Cell Host & Microbe (2023), https://doi.org/10.1016/j.chom.2023.11.020

Puromycin as a control. The lysates (0.5 mL) were layered on 4.4 mL of a 15% to 55% sucrose density gradient with 1.0 mg/mL Puromycin. Samples were centrifuged in a SW55Ti rotor (Beckman) at 45,000 rpm for 65 min at 4°C. 10 fractions (480 μL each) were collected after centrifuge. Fractions 1 to 10 were collected as progressive increase. RNA was isolated from each fraction and used for RT-PCR.

Immuno-isolation of EVs

The apoplastic wash fluids (AWF) were extracted from four-week-old *Arabidopsis* leaves by vacuum infiltration with buffer (20 mM 2-(N-morpholino) ethanesulfonic acid (MES), 2 mM $CaCl_2$, 0.1 M NaCl, pH 6.0) and centrifuged for 10 min at 900 *g*. Then it was cleaned by centrifugation at 2, 000 *g* for 20 min, filtered through a 0.22 or 0.45 μm filter, and centrifugation at 10,000 *g* for 30 min.[10] The cleaned AWF was used to obtain the EVs by centrifugation at 100,000 *g* for 1h (4 °C, Optima™ TLX Ultracentrifuge, Beckman Coulter, Indianapolis IN). The 100 000 *g* pellets (P100) were re-suspended in 500 μl immunoprecipitation (IP) buffer (50 mM Tris–HCl, pH 7.5; 150 mM NaCl, 10% glycerol, 1 mM DTT, 1 mM EDTA, proteinase inhibitor cocktail; Sigma). Protein A agarose beads were directly coupled to α-TET8 (10:1 (v/v)) by shaking incubation for 4-8 h at 4 °C. Free TET8 antibodies were removed with three times washing in IP buffer amended with 1 % Bovine Serum Albumin (BSA). Coupled agarose beads were well mixed with re-suspended pellets (1:20 v/v) and incubated for 4-8 h at 4 °C with gentle inverse shaking. The agarose beads were washed twice to remove non-specific binding, followed by RNA extraction or immunoblotting assay.

Immunoprecipitation and immunoblotting assays

α-GFP Nanobody/ V_HH conjugated to magnetic agarose beads (Chromotek) was used to immunoprecipitate RPL23-YFP from *B. cinerea* transformants expressing. Lysis buffer (10 mM Tris/Cl pH 7.5, 150 mM NaCl, 0.5 mM EDTA, 0.5 % Nonidet™ P40 Substitute, proteinase inhibitor cocktail; Sigma) was used to extract total protein using the manufacturer's protocol. 25 μl equilibrated beads were added into 1 mL and rotated end-over-end for 1.5 h at 4 °C, followed by beads-protein complex washing with wash buffer (10 mM Tris/Cl pH 7.5, 150 mM NaCl, 0.05 % Nonidet™ P40 Substitute, 0.5 mM EDTA) for three times. Beads were boiled for 10 min at 95 °C to dissociate immunocomplexes from beads for mass spectrometry or immunoblotting assay.

A. thaliana transgenic leaves or *N. benthamiana* leaves transiently expressing tagged fusion proteins were ground in liquid nitrogen, and resuspended in 2X sodium dodecyl sulfate–polyacrylamide gel electrophoresis (SDS-PAGE) sample loading buffer (100mM Tris, 4% SDS, 20 % glycerol, and 0.2 % bromophenol blue), and then separated on a 12 % SDS-PAGE gel with a 4 % stacking gel. Gel blotting onto nitrocellulose membrane, Ponceau staining, membrane blocking and washing steps were carried out as described by Mclellan et al.[76] α-mRFP primary antibody (Sigma-Aldrich) was used at 1: 2000 dilution, α-GFP antibody (Roche) was used to detect the YFP-fused proteins with 1: 2000 dilution. Secondary antibodies anti-mouse immunoglobulin G (IgG) horseradish peroxidase (HRP) or anti-rabbit IgG HRP (Abcam) were used at 1: 5000 dilutions. Native TET8, PR1 and Tic40 proteins were detected by rabbit polyclonal α-TET8 (1:1000 dilution), rabbit polyclonal α-PR1 (Agrisera, AS10687, 1:1000 dilution), rabbit polyclonal α-Tic40 (PhytoAB, PHY0461A, 1:2000 dilution) and rabbit polyclonal α-Tim17 (PhytoAB, PHY0536A, 1:2000 dilution) antibodies, respectively. Protein bands on immunoblots were detected using ECL substrate (Thermo Scientific Pierce, Rockford, IL, USA) using the manufacturer's protocol.

Nuclease and proteinase K protection assay

EVs were isolated from *A. thaliana* were treated with 10 U of micrococcal nuclease (MNase) or proteinase K to clarify whether mRNAs are protected by EVs. The detailed procedure was described previously.[26]

RT-PCR and gene expression analyses

RNA was extracted using TRIzol reagent according to the manufacturer's instructions. DNA contamination was removed using DNase I (Roche; 1 U μg^{-1} RNA at 37 °C for 30 min) based on the manufacturer's protocol. First-strand cDNA was synthesized by reverse transcription (RT) with Superscript III (Invitrogen) following the manufacturer's recommendations. Full- length plant mRNA transcripts were amplified from translation start code to stop code. Quantitative RT-PCR was carried out with the CFX384 real-time PCR detection system (Bio-Rad) using the SYBR Green mix (Bio-Rad). The primer sequences used in the reactions are listed in Table S5.

Confocal microscopy

Plant leaf pieces were mounted on slides and imaged using a Leica TCS SP5 confocal microscope (Leica Microsystems), and water dipping lenses. YFP was imaged with 514 nm excitation and emissions collected between 500 and 550 nm. Imaging of mCherry, FM4-64 and MITO-ID were conducted using 594 nm excitation and emissions were collected between 600 and 630 nm. 3WJ-4xBro was imaged with 488 nm excitation and emissions collected between 500 and 550 nm. *N. benthamiana* leaf tissue was usually imaged 2 d after *A. tumefaciens* infiltration, except imaging fusion transcripts tagged with *3WJ-4xBro in planta*, which was imaged after 4 days of infiltration. The leaves were incubated with 10 μM DFHBI-1T by infiltration for 16 h before imaging. For EV imaging, freshly prepared EVs fractions were incubated with 10 μM DFHBI-1T for 30 mins at room temperature.

Transmission electron microscopy (TEM)

Arabidopsis EVs were imaged using negative staining. Specifically, 10 μl of the EV sample was carefully deposited onto 3.0 mm copper Formvar-carbon-coated grids (TED PELLA) for 1 min. Excess sample was gently removed from the grids using filter paper to ensure optimal visualization. Following this, the grids were subjected to a staining process involving 1% uranyl acetate. Subsequently, the samples were allowed to air-dry before imaging. The JEM-1400plusTEM, operating at 100 kV, to capture high-resolution images of the EVs.

Nanoparticle Tracking Analysis (NTA)

We employed a NanoSight NS300 equipped with a blue laser operating at 405 nm and NanoSight NTA software version 3.1, developed by Malvern Panalytical. This advanced system allowed us to precisely assess the size distribution and concentration of EVs isolated from *Arabidopsis* leaves. The procedure involved diluting the EV samples by a factor of 50 with a phosphate-buffered saline solution. Subsequently, the diluted samples were introduced into the flow cell at a consistent flow rate of 50 units. To ensure robust and accurate measurements, four 60-second videos were recorded for each sample. These videos were then analyzed to determine the size distribution and concentration of the EVs.

Assay to measure transcript delivery and translation from EVs

EVs were isolated from uninfected transgenic *A. thaliana* lines expressing *SAG21-3WJ-4xBro*, *APS1-3WJ-4xBro*, *OEP6-3WJ-4xBro, SAG21-YFP, APS1-YFP, mSAG21-YFP,* or *mAPS1-YFP* fusion transcripts. *B. cinerea* conidia were collected from 10 days old PDA plates. 10^6 conidia were incubated in 200 μl RM medium for 4-5h at RT with gentle shaking. EVs which were isolated from transgenic plants expressing fused transcripts were treated with 30 μM DFHBI-1T for 30 mins before mixing with geminated conidia, then washed with 1ml KCl buffer containing 1% Triton X-100 three times before imaging or RNA extraction. Samples containing *YFP* transcripts were collected at 24 h before imaging or immunoblotting.

B. cinerea in vitro growth assay

B. cinerea transformants were maintained in PDA medium containing 50 μg/ml of hygromycin B. 10 μl droplets with concentration of 10^4/ml spores were inoculated on each 90 mm plate. The photos were took at 60 h.

RNA-seq and data analysis

Samples for RNA-seq: Col-0 leaves infected by *B. cinerea*; EVs isolated from Col-0 infected by *B. cinerea* or mock; TRAP of *Col-0* either infected or mixed with *in vitro* cultured *B. cinerea* transformants expressing *RPL23-YFP*. Total RNAs were extracted from the above samples using the TRIzol reagent and treated with DNase I. 1μg total RNAs from each sample was used for library preparation, NEB Next Poly(A) mRNA Magnetic Isolation Module kit (NEB #E7490) coupled with NEBNext® Ultra™ Directional RNA Library Prep Kit (NEB #E7420) were used to make libraries for Illumina sequencing based on the manufacturer's protocols. Data analysis: To assess and visualize the quality of raw reads, FastQC (https://www.bioinformatics.babraham.ac.uk/projects/fastqc/) and MultiQC[64] were applied. The RNA-seq data was of high quality and no trimming was required. RNAseq reads were mapped to a concatenated genome composed of *A. thaliana* (TAIR10) and *B. cinerea* B05 (ASM83294v1) using STAR (v. 2.7.5a).[65] The aligned reads were quantified at the gene level using the featureCounts function of the Rsubread package.[66] Ribosomal and other non-coding genes were filtered out from the analysis. The edgeR package in R[75] was used to perform differential gene expression analysis. Sample-type specific cutoffs and normalization strategies were performed as follows. TRAP libraries: genes with at least 100 CPM (counts per million) in all three libraries were kept. For *Arabidopsis* protein-coding genes RPKM expression values were calculated first using *Botrytis* ribosomal gene counts as a normalization factors. Differentially expressed genes were defined with a $\log_2$ fold-change significantly greater than 1.5 (using the glmTreat function)[77] and FDR-adjusted P-value < 0.05. At_Total and At_EVs libraries: genes with at least 3 CPM in all three libraries were condisered. The rpkm function of the edgeR package[47] was used to obtain normalized RPKM expression values. Signal peptides were predicted using the stand-alone software package of signalP (v. 5.0b).[68]

QUANTIFICATION AND STATISTICAL ANALYSIS

Ordinary one-way ANOVA using Dunnett's multiple comparisons test was used for statistical evaluation between multiple groups containing independent variables. The unpaired T-test was used for statistical evaluation between two groups. For all experiments, the exact number of experimental replicates was noted in the corresponding figure legends. Statistical analysis was performed using GraphPad Prism 9.3.1. P-values less than 0.05 were considered statically significant.